Lipid biomarker distributions in Oligocene and Miocene sediments from the Ross Sea region, Antarctica

Duncan, Bella; McKay, Robert; Bendle, James; Naish, Timothy; Inglis, Gordon N.; Moossen, Heiko; Levy, Richard; Ventura, G. Todd; Lewis, Adam; Chamberlain, Beth; Walker, Carrie

DOI:
10.1016/j.palaeo.2018.11.028

Lipid biomarker distributions in Oligocene and Miocene sediments from the Ross Sea region, Antarctica: Implications for use of biomarker proxies in glacially influenced settings

Bella Duncan[a], Robert McKay[a], James Bendle[b], Timothy Naish[a], Gordon N. Inglis[c], Heiko Moossen[b,d], Richard Levy[e], G. Todd Ventura[e,f], Adam Lewis[g], Beth Chamberlain[b,h], Carrie Walker[b,i].

[a]Antarctic Research Centre, Victoria University of Wellington, P.O. Box, Wellington 6012, New Zealand

[b]School of Geography, Earth and Environmental Sciences, University of Birmingham, Edgbaston, Birmingham, B15 2TT, UK

[c]Organic Geochemistry Unit, School of Chemistry and Cabot Institute, University of Bristol, Cantock's Close, Bristol BS8 1TS, UK

[d]Present address: Max Planck Institute for Biogeochemistry, P.O. Box 10 01 64, 07701 Jena, Germany

[e]Geological and Nuclear Sciences, P.O. Box 30-368, Lower Hutt 5040, New Zealand

[f]Present address: Department of Geology, Saint Mary's University, 923 Robie Street, Halifax, Nova Scotia, B3H 3C3, Canada

[g]North Dakota State University, Fargo, North Dakota, 58105, USA

[h]Present address: Department of Life Sciences, Imperial College London, Silwood Park Campus, Buckhurst Road, BioAscot, Berkshire, SL5 7PY, UK

[i]Present address: School of Environment, Earth and Ecosystem Sciences, The Open University, Milton Keynes, MK7 6AA, UK

Corresponding author: Bella Duncan, bella.duncan@vuw.ac.nz

Abstract

Biomarker-based climate proxies enable climate and environmental reconstructions for regions where other paleoclimatic approaches are unsuitable. The Antarctic Cenozoic record consists of widely varying lithologies, deposited in rapidly changing depositional settings, with large lateral variations. Previous sedimentological and microfossil studies indicate that the incorporation of reworked older material frequently occurs in these sediments, highlighting the need for an assessment of biomarker distribution across a range of depositional settings and ages to assess the role reworking may have on biomarker-based reconstructions. Here, we compare sedimentary facies with the distribution of *n*-alkanes and hopanoids within a terrestrial outcrop, two glaciomarine cores and a deep sea core, spanning the Late Oligocene to Miocene in the Ross Sea. Comparisons are also made with *n*-alkane distributions in Eocene glacial erratics and Mesozoic Beacon Supergroup sediments, which are both potential sources of reworked material. The dominant *n*-alkane chain length shifts from *n*-C_{29} to *n*-C_{27} between the Late Eocene and the Oligocene. This shift is likely due to changing plant community composition and the plastic response of *n*-alkanes to climate cooling. Samples from glaciofluvial environments onshore, and subglacial and ice-proximal environments offshore are more likely to display reworked *n*-alkane distributions, whereas, samples from lower-energy, lacustrine and ice-distal marine environments predominantly yield immature/contemporaneous *n*-alkanes. These findings emphasise that careful comparisons with sedimentological and paleontological indicators are essential when applying and interpreting *n*-alkane-based and other biomarker-based proxies in glacially-influenced settings.

Keywords: Paleoclimate, Antarctica, *n*-alkanes, biomarkers, hopanoids, reworking

1 Introduction

In Antarctic sediments, traditional microfossil-based methods of reconstructing climate can be challenging due to sparse distribution, low diversity of species, or poor preservation in sediments (i.e. Askin and Raine, 2000; Strong and Webb, 2000; Scherer et al., 2007). In contrast, biomarkers (molecular fossils preserved in the geological record) are relatively recalcitrant and have the potential to provide environmental proxy information when other methods are challenging or unsuitable. To date, only a few studies have employed biomarkers to investigate paleoclimate changes in Antarctica, with most of these conducted in offshore settings (i.e. Feakins et al., 2012; McKay et al., 2012; Pross et al., 2012; Bijl et al., 2013; Feakins et al., 2014; Levy et al., 2016; Rees-Owens et al., 2018). Such work is challenging because Cenozoic outcrops exposed in Antarctica are sparse, and are represented by relatively superficial and poorly-dated deposits of glacially derived tills, lacustrine and fluvial deposits, with occasional marine and glaciomarine sediments (Hambrey and Barrett, 1993; Marchant and Denton, 1996; Lewis et al., 2007; Lewis et al., 2008; Lewis and Ashworth, 2016). Sediments from drillcores on the continental margin are usually glaciomarine in origin and provide better-dated

records of cyclical fluctuations of the Antarctic Ice Sheets (Barrett, 1989; Naish et al., 2001, 2009). However, the variable lithologies in these sediments and the nature of their deposition mean that reworking of older sediments and associated fossil material is potentially a significant issue (e.g., Kemp and Barrett, 1975; Askin and Raine, 2000; Prebble et al., 2006a).

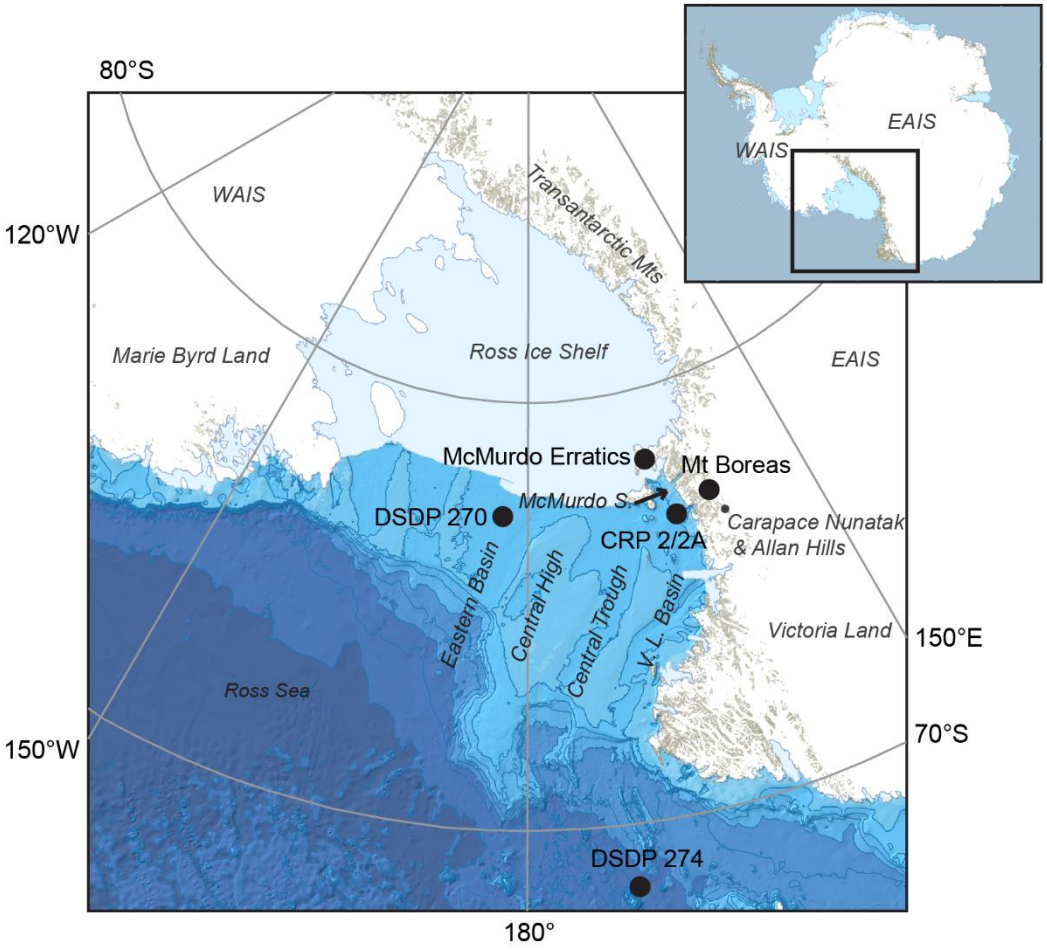

Fig. 1: Location of sample sites in the Ross Sea region of Antarctica. WAIS: West Antarctic Ice Sheet, EAIS: East Antarctic Ice sheet, DSDP: Deep Sea Drilling Project, CRP: Cape Roberts Project, McMurdo S.: McMurdo Sound, V.L. Basin: Victoria Land Basin. Base map from Quantarctica GIS package, Norwegian Polar Institute.

Here, lipid biomarkers (*n*-alkanes and hopanoids) are used to investigate how organic matter varies between different lithologies and depositional environments in the Ross Sea region of Antarctica. Specifically, we aim to assess whether lipid biomarkers represent organic material sourced from organisms living contemporaneously with sediment deposition, or older organic material which has been reworked into the sediment. Knowledge of potential reworking is critical for using and interpreting biomarker-based paleoenvironmental proxies in glacially-influenced settings. Localities and sediment drill cores were chosen to survey a range of depositional environments that together form a transect from high elevation terrestrial deposits to the deep sea (Fig. 1). These include; (i) A

Middle Miocene (~14 Ma) lacustrine/fluvial sequence from a small mountain glacier catchment at Mt Boreas in the Transantarctic Mountains. (ii) A Late Oligocene/Early Miocene glaciomarine sequence in the shallow marine Cape Roberts Project 2/2A drill core, sampling a coastal sediment catchment from an East Antarctic Ice Sheet (EAIS) outlet glacier. (iii) A deeper water Late Oligocene/Early Miocene glaciomarine sequence in DSDP Site 270 sampling sediment sourced from now submerged islands and ice caps in the central continental shelf of the Ross Sea, West Antarctica. (iv) An Early Miocene to Late Miocene marine sequence from DSDP Site 274 from the Western Ross Sea abyssal plain, sampling a wide sediment source catchment from both East and West Antarctica.

1.1 Geological setting

The western Ross Sea region of Antarctica is bounded by the Transantarctic Mountains (TAM), which were uplifted in the early Cenozoic, with the bulk of their exhumation occurring before the early Oligocene (Fitzgerald, 1994; Smellie, 2001). The basement rocks of the TAM are dominated by Archean to mid-Paleozoic metasediments and intrusives (Allibone et al., 1993a; Allibone et al., 1993b; Goodge et al., 2002). The Devonian to Triassic Beacon Supergroup overlies this basement (Barrett, 1981). Lithologies vary through the sequence, with interbedded sandstones, shales, conglomerates and coals deposited in a paleoenvironmental setting moving from shallow marine to a terrestrial system of lakes, braided rivers and alluvial plains (Barrett, 1981). Plant macrofossils and palynomorphs are common throughout the Beacon Supergroup (Barrett, 1981). In the early Jurassic, as the Gondwana super-continent began to separate, the Beacon Supergroup was intruded by the Ferrar Dolerite, resulting in extensive low grade thermal metamorphism (Barrett, et al., 1986). The Jurassic Ferrar Group contains extrusive volcanic rocks with fossiliferous sedimentary interbeds containing terrestrial microfossil assemblages (e.g. Ribecai, 2007).

Scattered sedimentary outcrops and the basaltic McMurdo Volcanic Group form the Cenozoic geology of the TAM (Marchant and Denton, 1996; Fielding et al., 2006; Martin et al, 2010). A significant Cenozoic sedimentary unit distributed throughout the TAM is the Sirius Group, which comprises glacial and non-glacial sediments with well-preserved fossil woody vegetation, leaf material and peat beds, deposited in terrestrial and proximal marine environments (Hambrey and Barrett, 1993; Francis and Hill, 1996; Barrett, 2013). Scattered Early Miocene to Holocene veneers of glacial tills, colluvium and lacustrine deposits are dispersed through the TAM (Marchant and Denton, 1996; Lewis et al., 2007; Lewis et al., 2008; Lewis and Ashworth, 2016). Eocene to Pliocene glacial erratics are found in the McMurdo region (Harwood and Levy, 2000). Much of what is currently known about Cenozoic Antarctic climate is based on seismic stratigraphy and continental margin drilling. Infill of sedimentary basins in the Ross Sea potentially began as early as the Late Cretaceous, with sediment accumulation continuing through the Cenozoic (Cooper et al., 1987; De Santis et al., 1995; Luyendyk et al., 2001; Decesari et al,, 2007; Wilson and Luyendyk, 2009). Continental margin

drill cores from the Ross Sea contain successions of subglacial, glaciomarine and marine sediments reflecting the cyclical advance and retreat of the Antarctic Ice Sheets (i.e. Barrett, 1989; Naish et al., 2001; Naish et al., 2009; McKay et al., 2009; Levy et al., 2016).

2 Methods

2.1 Site description

This work utilises samples from: (i) The McMurdo glacial erratics from the Mt Discovery and Minna Bluff region (Fig. 1), which yield marine and terrestrial micro- and macrofossils of mid-late Eocene age and are interpreted as being deposited in coastal-terrestrial and nearshore marine environments, under ice-free conditions (Harwood and Levy, 2000). (ii) Mid-Miocene terrestrial, fossil-bearing strata from Mt Boreas in the Olympus Range, which record the last known vestige of vegetation in the TAM before the Dry Valleys transitioned from wet- to cold-based glaciation at high altitudes (1,425 m) (Fig. 1) (Lewis et al., 2008). (iii) Oligocene/Early Miocene glaciomarine sediments obtained from the Cape Roberts Project core CRP-2/2A from the Victoria Land continental slope of Antarctica (Fig. 1) (Cape Roberts Science Team, 1999). (iv) A Late Oligocene to Early Miocene glaciomarine sequence of sediments from DSDP Site 270, drilled on the continental shelf in the central Ross Sea in 1973 and re-described in 2015 (Fig. 1) (The Shipboard Scientific Party, 1975a; Kraus, 2016). (v) An Early to Late Miocene succession of ice-distal diatom-rich silty clay sediments from DSDP 274 on the lower continental rise in the northwestern Ross Sea (68°59.81'S, 173°25.64'W) (Fig. 1) (The Shipboard Scientific Party, 1975b). Figure 2 schematically describes the sampling sites and facies used in this study.

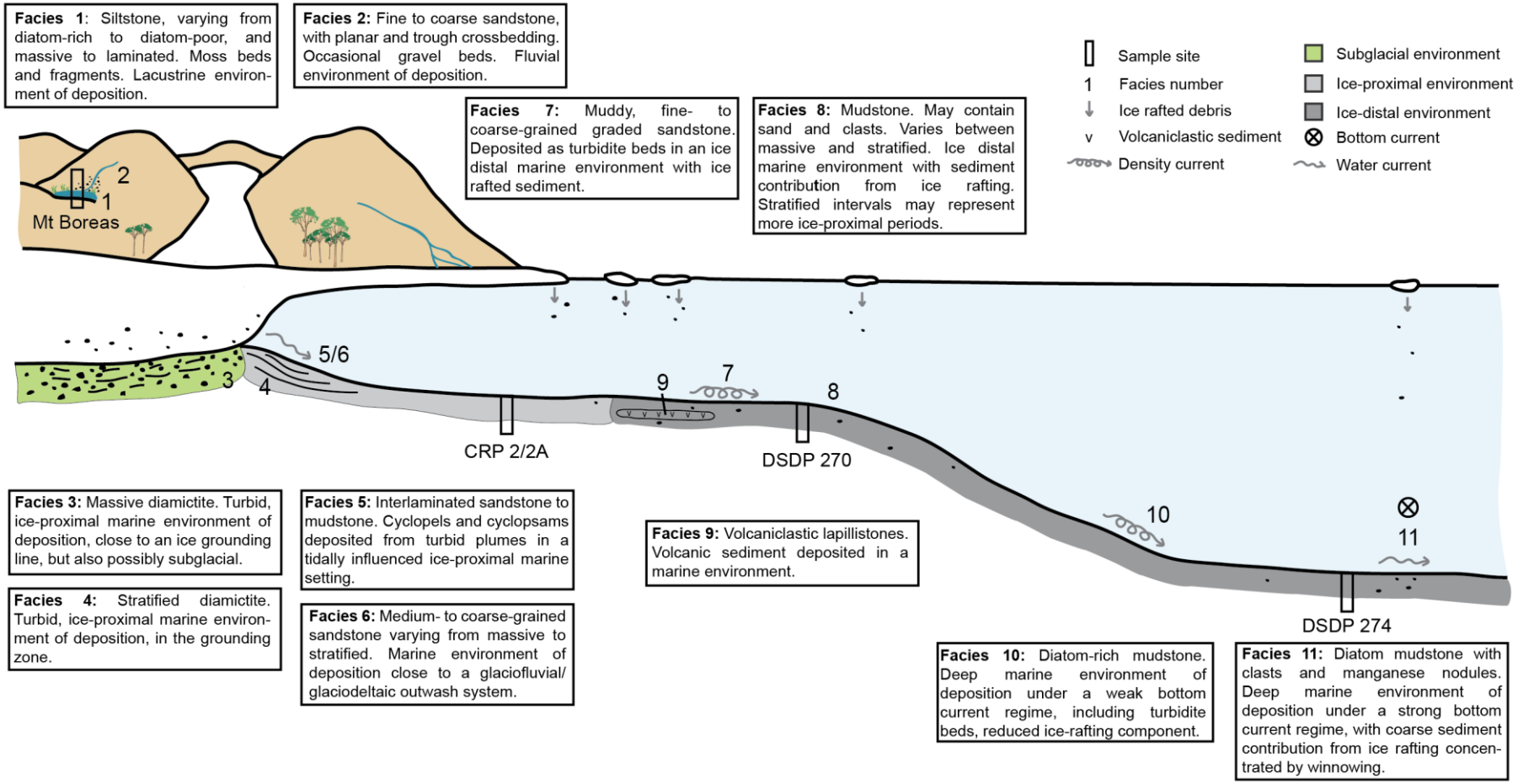

Fig. 2. Schematic representation of Oligocene and Miocene environments of deposition in the Ross Sea Region, and their associated sedimentary facies. Sample sites are placed in their representative depositional setting.

142

143 *2.2 Bulk analysis*

144 Unless already desiccated, samples were freeze dried for 48 h prior to sample work up. All
145 samples were homogenised to a powder using a Retsch 200 mixer mill.

146 Pyrolysis measurements for total organic carbon (TOC) were made using a Weatherford
147 laboratories Source Rock Analyzer at GNS Science on ~100 mg of powdered sediment. The
148 pyrolysis program was set with the sample crucible entering the pyrolysis oven where it was held
149 isothermal at 300 °C for 3 mins under a continuous stream of He carrier gas using a 100 ml/min flow
150 rate. This was followed by a 25 °C/min ramp to 650 °C. The S1 and S2 signal intensities were
151 recorded with a FID operated under a 65 ml/min stream of H_2 gas and 300 ml/min air. The pyrolysis
152 cycle was then followed by an oxidation cycle performed at 630 °C for 20 mins during which time the
153 oven and crucible were flushed with dry air at 250 ml/min. The generated carbon monoxide and
154 carbon dioxide gases were measured by the instrument's IR cells. All sample sequences were run
155 with three IFP 160000 analytical standard replicates (from Vinci Technologies, Institut Français du
156 Pétrole) placed at the beginning, middle and end of each sample sequence.

157 *2.3 Lipid biomarker analyses*

158 Organic geochemical work-up, gas chromatograph (GC)-flame ionization detector (FID) and
159 GC-Mass Spectrometer (MS) analyses was performed in the Birmingham Molecular Climatology
160 Laboratory (BMC), University of Birmingham. Lipids were extracted from ~10-15 g of homogenised
161 sediment by ultrasonic extraction using dichloromethane (DCM):methanol (3:1). The total lipid
162 extract was fractionated by silica gel chromatography using *n*-hexane, *n*-hexane:DCM (2:1), DCM,
163 and methanol to produce four separate fractions, the first of which contained the aliphatic saturated
164 and unsaturated hydrocarbons (e.g. *n*-alkanes, steranes and hopanes). Procedural blanks were also
165 analysed to ensure the absence of laboratory contaminants.

166 The aliphatic hydrocarbon fractions were analysed on an Agilent 7890B series GC, equipped
167 with a 7639ALS autosampler, a BP5-MS column (SGE Analytical Science, 60 m × 0.32 mm × 0.25
168 μm) and an FID, using hydrogen (H_2) as a carrier gas. Compound separation was achieved by using
169 the following temperature program: the oven was held at 70 °C for 1 min, then heated to 120 °C at 30
170 °C/min, and then to 320 °C with 3 °C/min, where it was held for 20 mins. GC-Mass spectrometry
171 (GC-MS) was performed using an Agilent 7890B GC, coupled to an Agilent 5977A Mass Selective
172 Detector (MSD). The same capillary column and temperature program was used throughout the
173 analyses for consistent compound separation. Helium (He) was used as a carrier gas. Samples were
174 bracketed with an external standard containing known abundances of certain *n*-alkanes to allow
175 identification and quantification of *n*-alkanes (average standard deviation of ± 7.6%). *n*-Alkane peaks

were integrated in Agilent OpenLAB Data Analysis Version A.01.01 - Build 1.93.0. Relationships between *n*-alkane indices were investigated using Pearson's correlation coefficients and assessed as statistically significant when $p<0.05$. Hopanes and hopenes were identified based upon published spectra, characteristic mass fragments and retention times (e.g. Rohmer et al., 1984; Sessions et al., 2013; Inglis et al., 2018) and integrated using GC-MS.

2.4 Biomarker indices

n-Alkanes of specific carbon chain lengths are known to be derived from discrete biological sources. Algae and some photosynthetic bacteria typically produce dominantly *n*-C_{17}, with lesser amounts of *n*-C_{15} and *n*-C_{19} (Clark and Blumer, 1967; Han and Calvin, 1969; Cranwell et al., 1987). Other species of bacteria, including non-photosynthetic bacteria often demonstrate an even carbon number preference between *n*-C_{12} and *n*-C_{22}, commonly with high *n*-C_{16} and *n*-C_{18} (Han and Calvin, 1969; Grimalt and Albaigés, 1987). Non-emergent aquatic plants and *Sphagnum* mosses show enhanced production of *n*-C_{23} and *n*-C_{25} (Baas et al., 2000; Ficken et al., 2000; Pancost et al., 2002; Bingham et al., 2010). Long chain *n*-alkanes (*n*-C_{25} and higher), usually with a high odd-over-even predominance, are most abundant in the epicuticular waxes on leaves and stems of terrestrial higher plants (Eglinton and Hamilton, 1963). *n*-Alkanes are also derived from the early diagenetic alteration of saturated and unsaturated aliphatic alcohols, ketones, esters, and di- or triterpenic acids (i.e. Tissot and Welte, 1984; Meyers and Ishiwatari 1993). Once deposited, *n*-alkanes may undergo microbial or geochemical alteration, modifying their distributions (Grimalt et al., 1985).

The source and maturity of higher molecular weight *n*-alkanes can be characterised by their carbon preference index (CPI):

$$CPI = \frac{1}{2}\left(\left(\frac{\Sigma_{odd}(n-C_{25-33})}{\Sigma_{even}(n-C_{24-32})}\right) + \left(\frac{\Sigma_{odd}(n-C_{25-33})}{\Sigma_{even}(n-C_{26-34})}\right)\right) \quad (1)$$

Most modern sediments with terrestrially sourced organic matter have an odd-over-even predominance of long chained *n*-alkanes (*n*-C_{25} to *n*-C_{34}) and CPI values >1 (Bray and Evans, 1961; Eglinton and Hamilton, 1963). A survey of modern leaf wax material demonstrates that a CPI of >1-2 is a reasonable threshold value indicative of relatively unmodified terrestrial plant material (Bush and McInerney, 2013). Sediments containing CPI values of <1 usually indicate either exposure to elevated burial temperatures great enough to cause hydrocarbon cracking, or an input of organic matter that has been altered by diagenetic or catagenetic processes (Bray and Evans, 1961). Some sediments will also display an unresolved complex mixture (UCM), represented by a hump in the baseline of a gas chromatogram due to the co-elution of unresolved compounds (Gough and Rowland, 1990; Gough et al., 1992). UCMs can be especially prominent in biodegraded petroleums, in which microbial degradation of the more abundant aliphatic components leads to increased concentrations of the more recalcitrant, branched and cyclic compounds (Gough and Rowland, 1990; Gough et al., 1992). In

recent sediments, *n*-alkanes have a lower susceptibility to microbial degradation than most other types of organic matter as they lack functional groups, but studies on peat and lake sediments suggest that microbial degradation does occur (Meyers and Ishiwatari, 1993; Lehtonen and Ketola, 1993). Shorter chain lengths appear more degradable than longer chain lengths, and microbial degradation can result in a decrease in CPI (Meyers and Ishiwatari, 1993; Lehtonen and Ketola, 1993).

Average chain length (ACL) indicates the dominant *n*-alkane in a given carbon number range (Poynter et al., 1989; Schefuß et al., 2003):

$$ACL = \frac{\Sigma(C_{odd\ 25-33} \cdot x_{odd\ 25-33})}{(x_{odd\ 25-33})} \quad (2)$$

Where $C_{odd\ 25\text{-}33}$ represents the carbon number of the odd chain length *n*-alkanes, and $x_{odd\ 25\text{-}33}$ represents the concentrations of the odd *n*-alkanes in the sample. ACL is influenced by a number of factors. Higher ACLs are typical of warmer, tropical regions, whilst lower ACLs are more commonly observed from cooler, temperate regions, indicating that ACL could be related to air temperature (Gagosian and Peltzer, 1986; Poynter et al., 1989; Dodd and Afzal-Rafii, 2000; Kawamura et al., 2003; Bendle et al., 2007; Vogts et al., 2009; Bush and McInerney, 2015). Other studies have suggested that aridity has a strong control on ACL, with the synthesis of longer *n*-alkanes in more arid environments providing plants with a more efficient wax coating to restrict water loss (Dodd et al., 1998; Dodd and Afzal-Rafii, 2000; Schefuß et al., 2003; Calvo et al., 2004; Zhou et al., 2005; Moossen et al., 2015). ACL is also strongly controlled by the contributing vegetation, with large inter- and intra-species variation in *n*-alkane distributions (i.e. Vogts et al., 2009; Bush and McInerney, 2013; Feakins et al., 2016). Variation in average chain length through time therefore reflects the interplay of two key factors: climate-driven plastic response of *n*-alkanes to temperature and/or aridity within a plant community; or changes to the composition of the plant community, often in response to climate (Bush and McInerney, 2013).

Hopanes and hopenes are C_{27} to C_{35} pentacyclic triterpenoids derived from a wide range of bacteria (Rohmer et al., 1984; Talbot and Farrimond, 2007). Hopanes are ubiquitous across a variety of depositional settings, and in both modern and ancient sediments (Ourisson and Albrecht, 1992). In modern sediments, hopanes are mostly present in the biological 17β,21β(H) configuration (although there are exceptions; see Inglis et al., 2018). In sediments, with increasing diagenesis, hopanes undergo stereochemical transformations and the biologically-derived 17β,21β(H)-hopanoid is transformed into the more thermally stable 17β,21α(H) and 17α,21β(H)-stereoisomers (Mackenzie et al., 1980; Peters and Moldowan, 1991). With increasing maturation, extended hopanoids ($>C_{30}$) also undergo isomerisation at the C-22 position. As such, hopanoids are frequently used to reconstruct thermal maturity (Mackenzie et al., 1980; Seifert and Moldowan, 1980; Peters and Moldowan, 1991; Farrimond et al., 1998), where decreasing ββ/(αβ+βα+ββ) indices and increasing 22S/(22R + 22S) values indicate increasing thermal maturity. The ratio of C_{27} 18α(H)-trisnorhopane II (Ts) to C_{27}

17α(H)-trisnorhopane (Tm) is also commonly used as a maturity parameter, as Tm is less stable during catagenesis than Ts (Seifert and Moldowan, 1978).

3 Results

3.1 Facies compilation

In order to compare results between sites, an internally consistent facies scheme was developed based on published facies descriptions for each sample site (Fig. 2). The McMurdo erratics were not included, as the context and relationship between these samples is uncertain. Instead these samples were labelled by lithofacies as described by Levy and Harwood (2000) (Supplementary table 1). Samples from Mt Boreas were assigned facies based on descriptions from Lewis et al. (2008). Facies for CRP 2/2A were developed based on descriptions of Fielding et al. (2000). Facies for DSDP 270 were assigned using descriptions of Kraus (2016), and based on previous models of glaciomarine facies successions (Fielding et al, 2000; Powell and Cooper, 2002; McKay et al., 2009). For DSDP 274, facies were determined by using interpretations from The Shipboard Scientific Party (1975b), Frakes (1975) and Whittaker and Müller (2006).

3.2 McMurdo erratics

Six Mid- Late Eocene sediment samples from the McMurdo erratics suite were analysed for *n*-alkanes, sourced from a range of lithofacies (Levy and Harwood, 2000) (Supplementary table 1). Three of the samples (E214, MB245 and E215) are dominated by the *n*-C_{17} to *n*-C_{20} short chained *n*-alkanes underlain by a UCM (Fig. 3). Samples D1, E219 and MTD95 have bimodal profiles, dominated by ~*n*-C_{20} to *n*-C_{23} underlain by small a UCM, and a series of longer *n*-alkanes with a mode at ~*n*-C_{29} (Fig. 3). In all samples, *n*-C_{29} is the dominant long-chained *n*-alkane, in contrast to younger strata investigated in this study usually dominated by *n*-C_{27}. The ratio between these two chain lengths has been described at all sites to investigate its variance at other localities. The CPI from the McMurdo Erratics ranges from 1.8 to 5.5 (avg. 2.8). ACL varies from 27.9 to 28.7 (avg. 28.2), whilst the ratio of the *n*-C_{29} *n*-alkane to *n*-C_{27} ranges from 1.01 to 1.64 (avg. 1.26). The erratics contain total abundances of *n*-alkanes ranging from 83 μg/gTOC to 1579 μg/gTOC, at an average of 406 μg/gTOC.

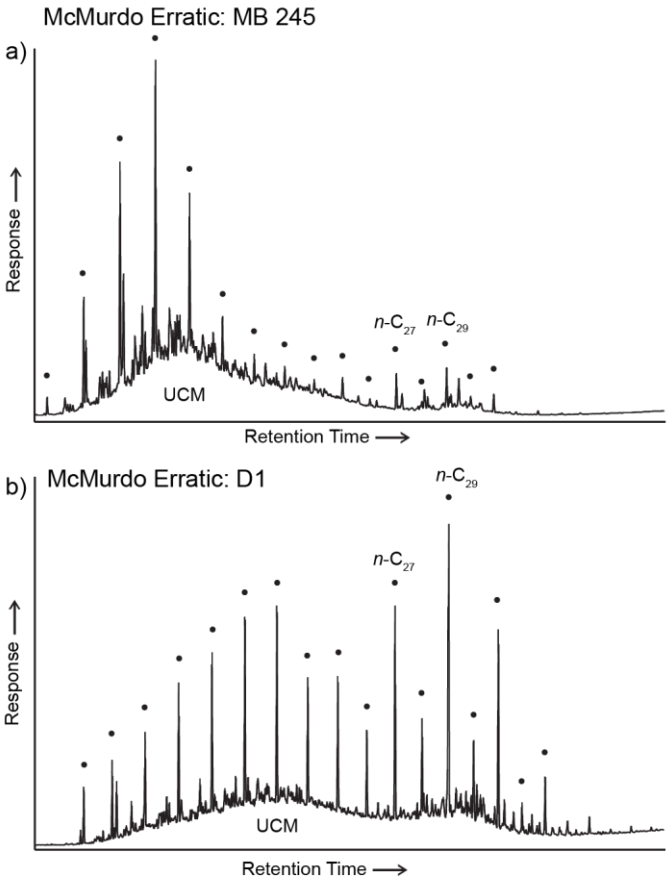

Fig. 3. Representative GC-FID-chromatograms of two samples of the McMurdo erratics. Filled circles above peaks indicate n-alkanes, with the n-C_{27} and n-C_{29} labelled. UCM: unresolved complex mixture.

3.3 Mt Boreas

12 sediment samples from Mt Boreas were analysed for *n*-alkanes (Supplementary table 1) Samples from Mt Boreas are typically dominated by long chained *n*-alkanes, particularly *n*-C_{23}, *n*-C_{25} and *n*-C_{27} (Fig. 4). Some samples display small UCMs, usually underlying ~*n*-C_{19} to *n*-C_{20}. Samples were collected from three different sites within a topographic depression which held a small alpine line, from units that are correlatable to the stratigraphic column shown in Figure 4 (Lewis et al., 2008). The total abundance of *n*-alkanes at these sites ranges between 4.5 μg/gTOC to 762 μg/gTOC, at an average of 206.5 μg/gTOC. The CPI of the long-chained *n*-alkanes ranges from 1.7 to 5.9 (avg. 3.4), whilst ACL varies from 26.2 to 27.4 (avg. 26.9). The ratio of the *n*-C_{29} *n*-alkane to *n*-C_{27} varies from 0.15-0.97 (avg. 0.55), indicating that the *n*-C_{27} dominates the *n*-C_{29} in all samples from these sites (Supplementary table 1).

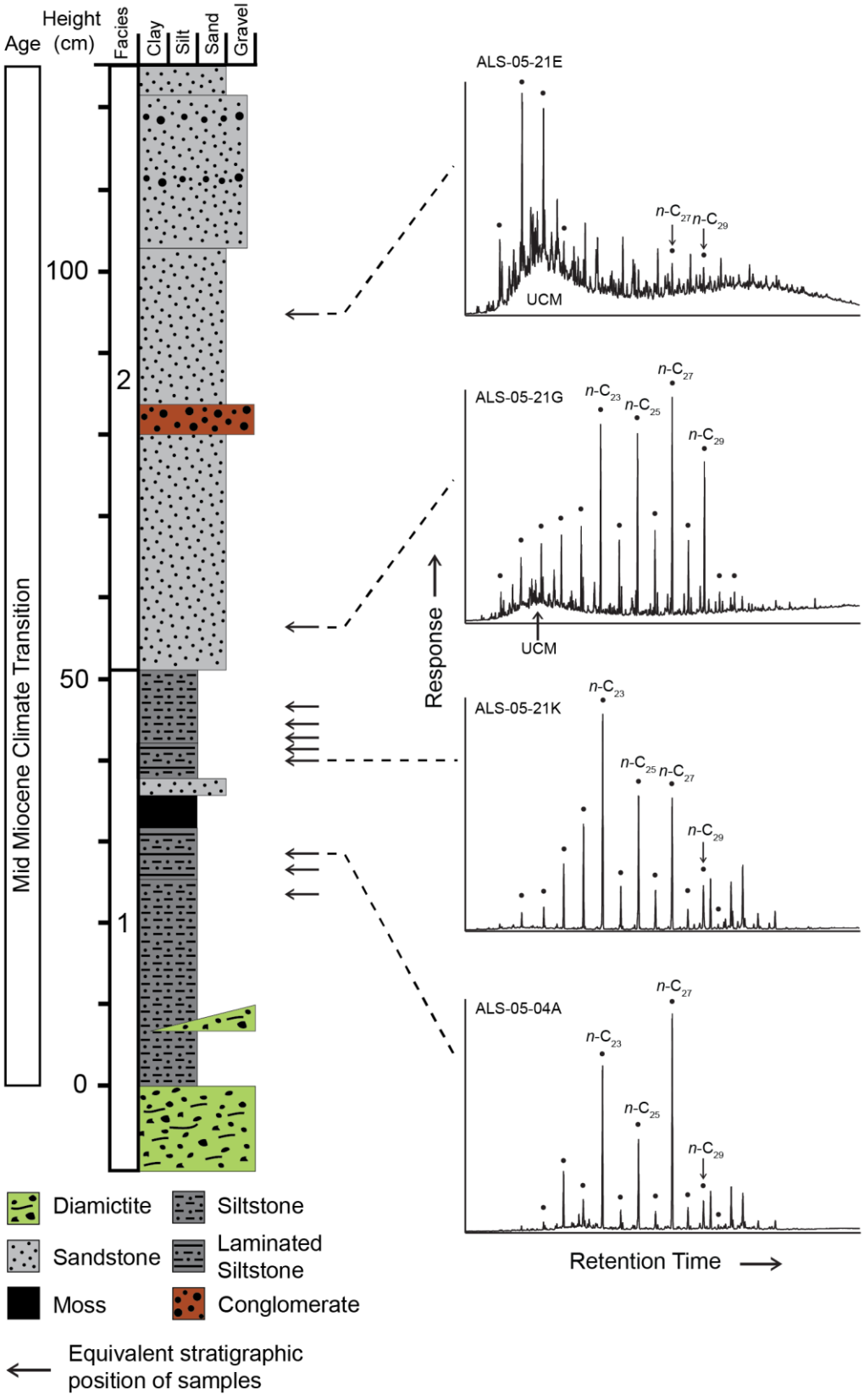

287

288 *Fig. 4. Stratigraphic column from a site at Mt Boreas (after Lewis et al., 2008) with the*
289 *equivalent stratigraphic positions of representative GC-FID-chromatograms of samples. Filled*

circles above peaks indicate n-alkanes, with the n-C_{27} and n-C_{29} labelled. Facies numbers are described in Fig. 2. UCM: unresolved complex mixture.

Pearson's correlation coefficients were estimated for each *n*-alkane variable compared to other *n*-alkane variables from these sites. Only two variables demonstrate a statistically significant correlation to each other; the ratio of *n*-C_{29}/*n*-C_{27} typically decreases with increasing CPI (r = 0.711, p = 0.0096) (Fig. 5). Samples from fluvial Facies 2 typically display lower CPI, and higher ACL and *n*-C_{29}/*n*-C_{27} values than those from lacustrine Facies 1, although it is noted that the Facies 2 is only represented by two samples (Fig. 6). Both fluvial and lacustrine samples show similar average total abundances of *n*-alkanes.

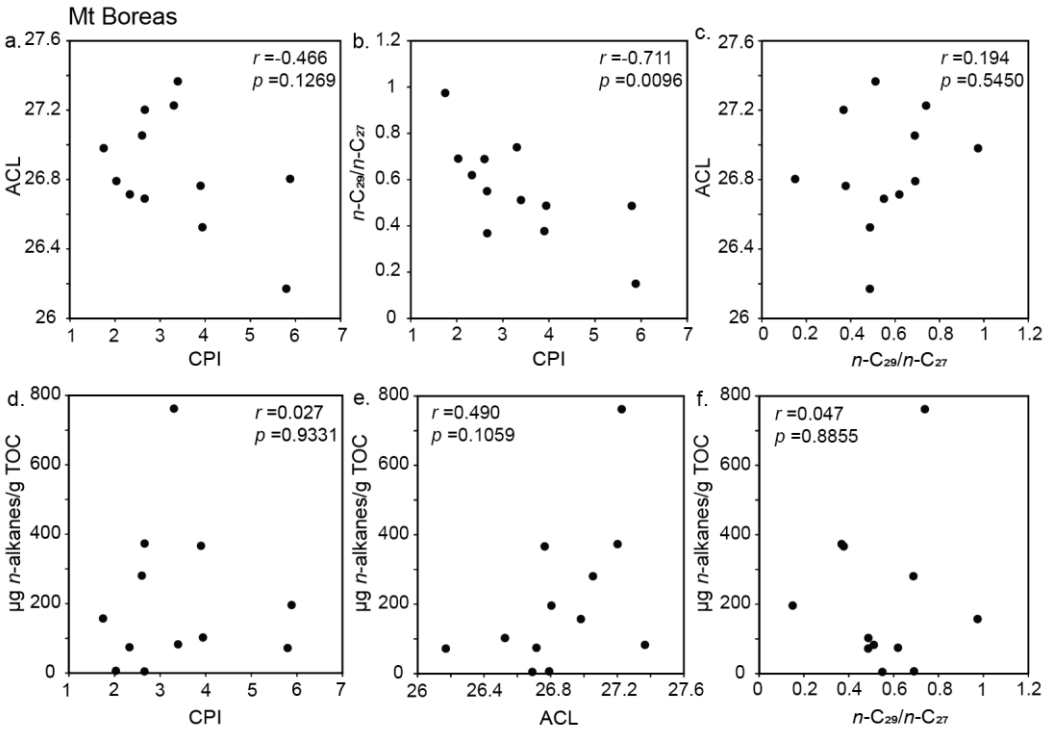

Fig. 5. Scatter plots of samples from Mt Boreas; a) CPI and ACL; b) CPI and n-C_{29}/n-C_{27}; c) n-C_{29}/n-C_{27} and ACL; d) CPI and the total abundance of n-alkanes (µg n-alkanes/g TOC); e) ACL and the total abundance of n-alkanes (µg n-alkanes/g TOC) and f) n-C_{29}/n-C_{27} and the total abundance of n-alkanes (µg n-alkanes/g TOC).

Three samples representing typical *n*-alkane distributions from the site were also analysed for additional biomarkers (Supplementary table 2). In two samples (ALS-05-21N and ALS-05-04C), hopanoids were abundant and the distribution was dominated by 17β(H)-trisnorhopane (C_{27}) and 17β,21β(H)-norhopane (C_{29}). Both samples are characterised by high ββ/(αβ+βα+ββ) ratios (0.82 to 0.86) and indicate low thermal maturity. Within sample ALS-05 21O, hopanoids were weak and the distribution was dominated by thermally-mature C_{27} to C_{35} hopanes. This sample was characterised by

a low ββ/(αβ+βα+ββ) ratio (0.07) and high C22S/C22R+C22S ratio (0.58) and therefore indicate high thermal maturity.

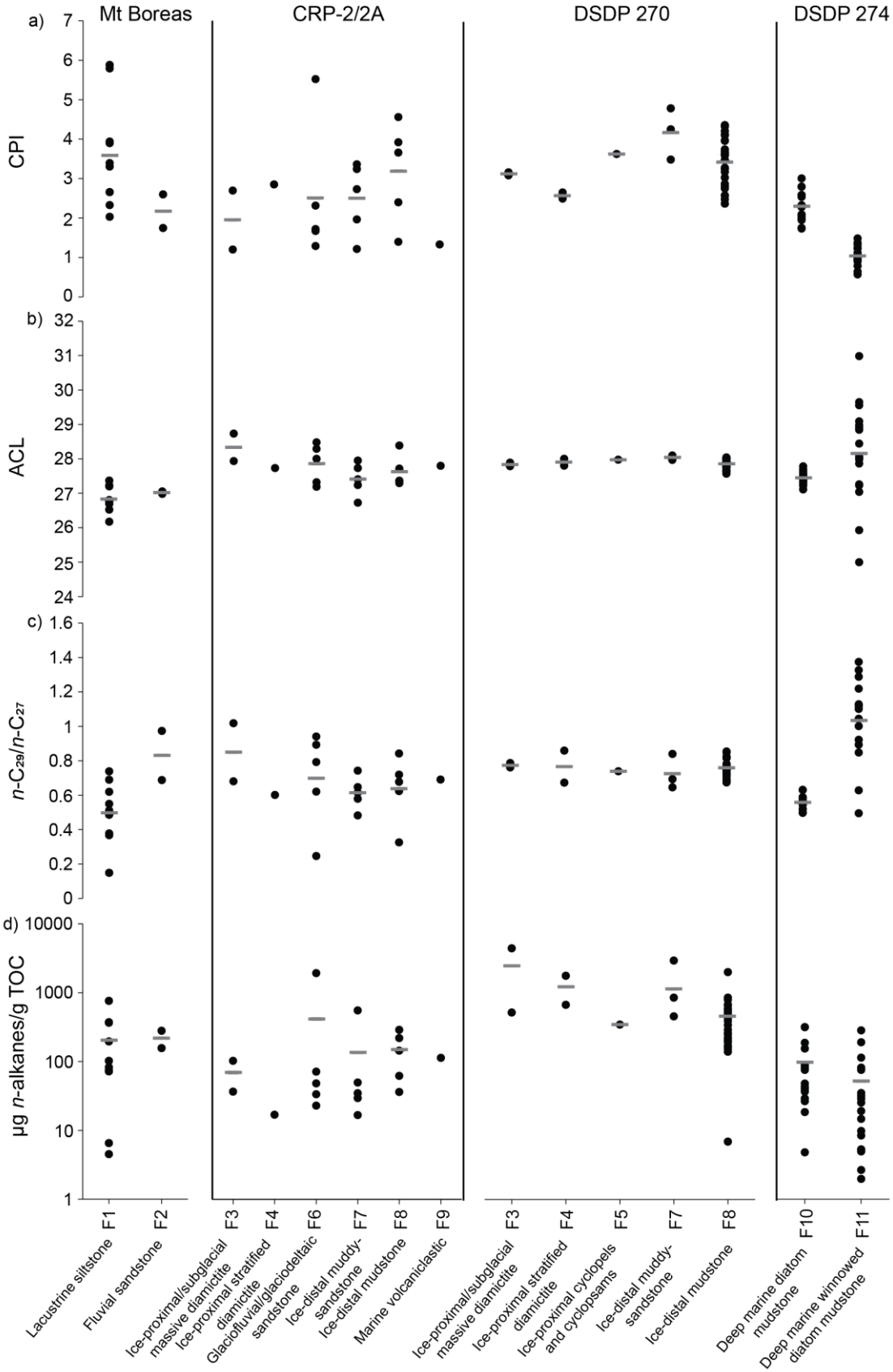

Fig. 6: Distributions of n-alkane variables across different facies from Mt Boreas, CRP-2/2A, DSDP 270 and DSDP 274; a) CPI, b) ACL, c) n-C_{29}/n-C_{27} and d) the total abundance of n-alkanes (μg n-alkanes/g TOC). Grey bars represent average values for each facies. Description of facies in Fig. 2.

3.4 Cape Roberts Project 2/2A

Long chained *n*-alkanes typically dominate samples from CRP 2/2A (Fig. 7). The *n*-C_{23}, *n*-C_{25} and *n*-C_{27} are usually the most abundant homologs, with *n*-C_{27} often the most prominent of these. In some samples *n*-alkanes elute with a UCM, which is usually centred between *n*-C_{19} and *n*-C_{23}. The total abundance of *n*-alkanes is highly variable from sample to sample, ranging from 16.6 μg/gTOC to 1893.0 μg/gTOC, averaging 197.6 μg/gTOC. CPI also varies over a wide range, from 1.2-5.5 (avg. 2.6), whilst ACL ranges from 26.7-28.7 (avg. 27.7). The ratio of the *n*-C_{29} *n*-alkane to *n*-C_{27} varies from 0.25-1.02 (avg. 0.67) (Supplementary table 1).

Pearson's correlation coefficient estimations show statistically significant correlations between several *n*-alkane variables. The strongest correlations exist between CPI and *n*-C_{29}/*n*-C_{27} (r = 0.837, $p < 0.0001$) and ACL and *n*-C_{29}/*n*-C_{27} (r = 0.777, $p < 0.0001$), with a weaker correlation between CPI and ACL (r = 0.580, p = 0.0091). Figure 8 shows that at both high and low values of CPI and *n*-C_{29}/*n*-C_{27}, the total abundance of *n*-alkanes increases, with weak correlations between these variables (r = 0.516, p = 0.0238 and r = 0.520, p = 0.0225, respectively). Most facies contain a range of both high and low values of CPI, with the highest average CPI in the low-energy marine mudstones of facies 8 (Fig. 6). Facies 6, 7 and 8 also have broad ranges of ACL and *n*-C_{29}/*n*-C_{27}, with the lowest average ACL and *n*-C_{29}/*n*-C_{27} in the poorly sorted sandstones of facies 7, while facies 3, consisting of massive diamictites, has the highest average ACL and *n*-C_{29}/*n*-C_{27}. Two samples containing a much higher concentration of *n*-alkanes than other samples in the facies skew the averages for facies 6 and 7. Without these outliers, facies 8 contains the highest average total abundance of *n*-alkanes.

Additional biomarkers were investigated in two samples, with a range of C_{27}–C_{32} hopanes and C_{27}–C_{30} hopenes were present (Supplementary table 2). The dominant compound was 17β,21β(H)-bishomohopane (C_{32}) or 17α,21β(H)-hopane (C_{30}) and samples were characterised by low-to-moderate ββ/(αβ+βα+ββ) ratios (0.45 to 0.65). As such, these samples are characterised by relatively low thermal maturity.

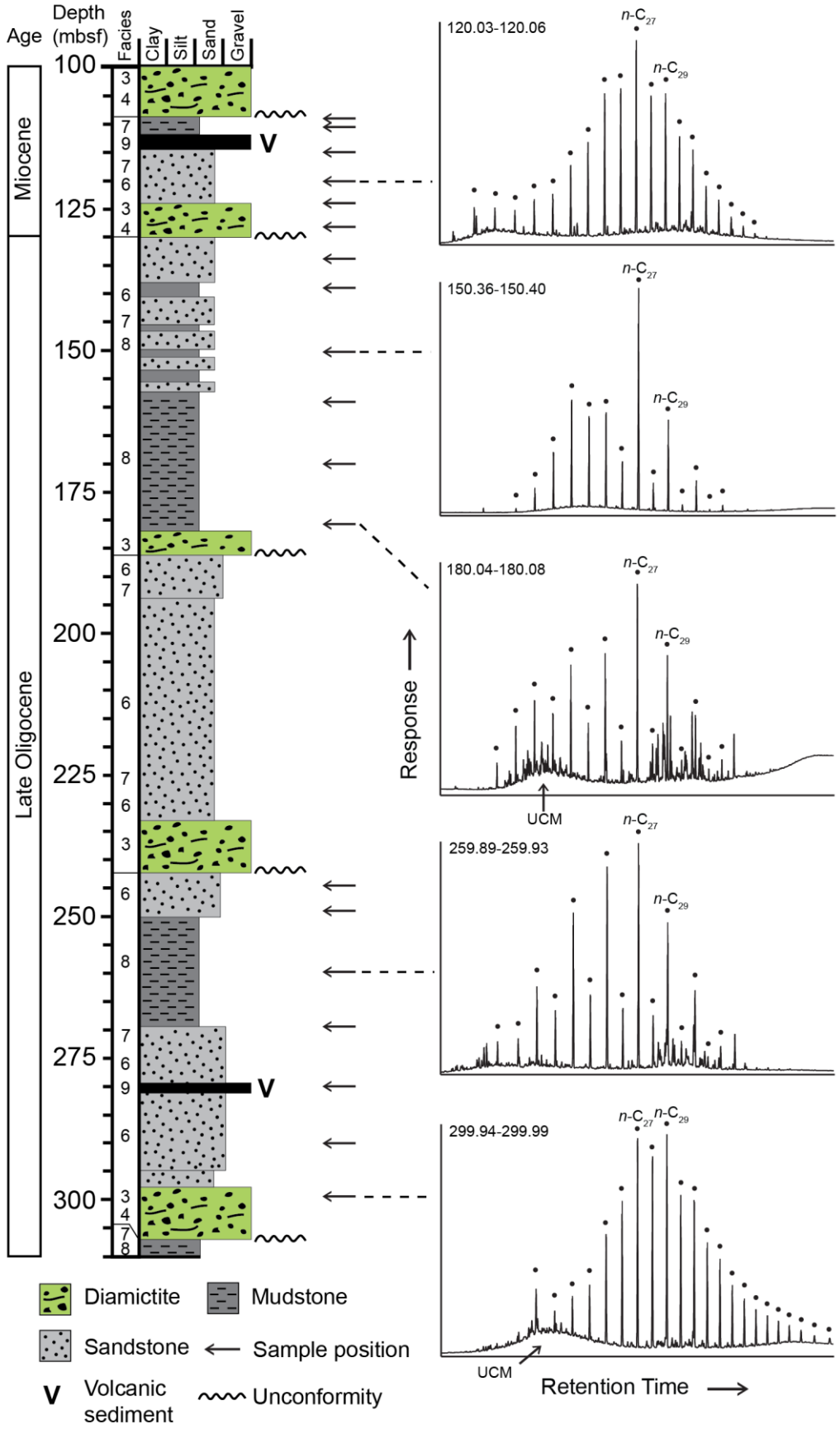
Age
Depth (mbsf)
Facies
Clay
Silt
Sand
Gravel
Miocene
Late Oligocene
100
125
150
175
200
225
250
275
300
V
120.03-120.06
150.36-150.40
180.04-180.08
259.89-259.93
299.94-299.99
n-C27
n-C29
UCM
Response
Retention Time
Diamictite
Mudstone
Sandstone
Sample position
Volcanic sediment
Unconformity

342

Fig. 7. Stratigraphic column from CRP 2/2A with the stratigraphic positions of representative GC-FID-chromatograms of samples. Filled circles above peaks indicate n-alkanes, with the n-C_{27} and n-C_{29} labelled. Simplified facies groupings are labelled, and are described in table 1. UCM: unresolved complex mixture.

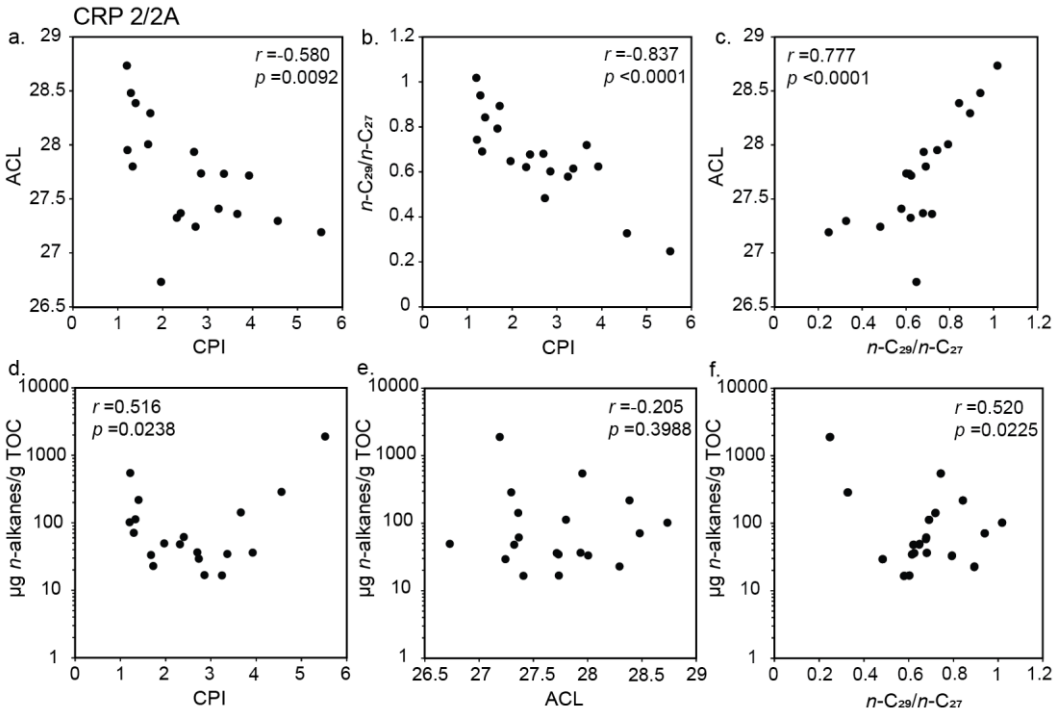

Fig. 8. Scatter plots of samples from CRP 2/2A; a) CPI and ACL; b) CPI and n-C_{29}/n-C_{27}; c) n-C_{29}/n-C_{27} and ACL; d) CPI and the total abundance of n-alkanes (µg n-alkanes/g TOC); e) ACL and the total abundance of n-alkanes (µg n-alkanes/g TOC) and f) n-C_{29}/n-C_{27} and the total abundance of n-alkanes (µg n-alkanes/g TOC).

3.4 DSDP 270

Samples from DSDP 270 typically display bimodal *n*-alkane distributions with a peak at *n*-C_{17} or *n*-C_{19} and another peak *n*-C_{27} (Fig. 9). Shorter chained *n*-alkanes (> *n*-C_{20}) are usually more abundant than the long chained homologs, and in four samples from the lowest sampled section of the core, long chained *n*-alkanes were not detected. Some samples display a small UCM underlying ~*n*-C_{20} and *n*-C_{21}. CPI of the long chained *n*-alkanes ranges from 2.4-4.8 (avg. 3.4). ACL varies from 27.6-28.1 (avg. 27.9), whilst the ratio of *n*-C_{29} to *n*-C_{27} ranges from 0.65-0.86 (avg. 0.76). The samples have an average total abundance of *n*-alkanes of 680.92 µg/gTOC (Supplementary table 1).

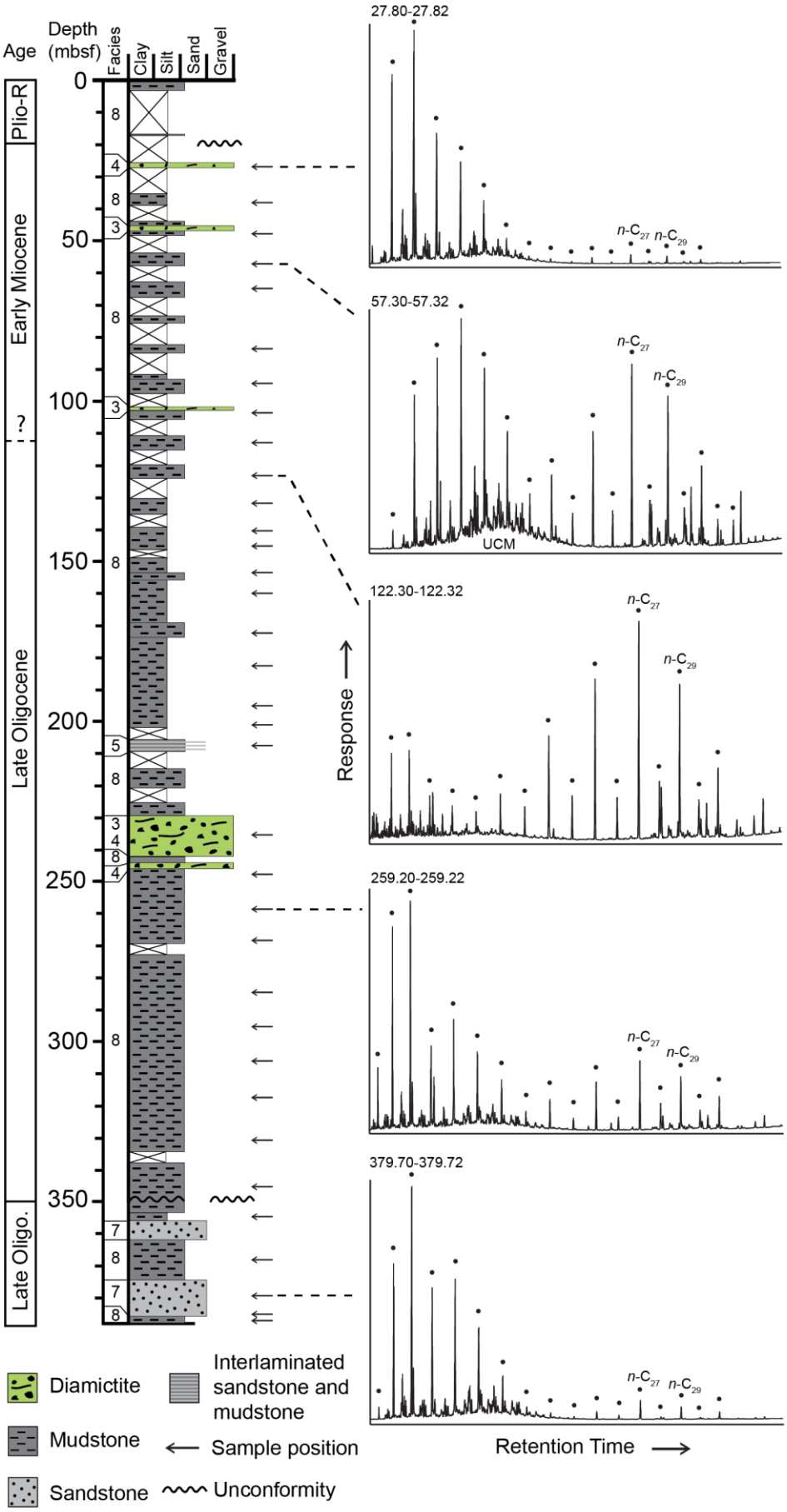
Age
Depth (mbsf)
Facies
Clay
Silt
Sand
Gravel
Plio-R
Early Miocene
?
Late Oligocene
Late Oligo.
0
50
100
150
200
250
300
350
27.80-27.82
57.30-57.32
122.30-122.32
259.20-259.22
379.70-379.72
n-C27
n-C29
UCM
Response
Retention Time
Diamictite
Mudstone
Sandstone
Interlaminated sandstone and mudstone
Sample position
Unconformity

Fig. 9. Stratigraphic column from DSDP 270 with the stratigraphic positions of representative GC-FID-chromatograms of samples. Filled circles above peaks indicate n-alkanes, with the n-C_{27} and n-C_{29} labelled. Simplified facies groupings are labelled, and are described in table 1. UCM: unresolved complex mixture.

Pearson's correlation coefficients show no particularly strong correlations between *n*-alkane variables. Increasing *n*-C_{29}/*n*-C_{27} with decreasing CPI is very weakly correlated ($r = 0.391$, $p = 0.0221$), with a slightly stronger correlation existing between decreasing *n*-C_{29}/*n*-C_{27} with decreasing ACL ($r = 0.533$, $p = 0.0012$) (Fig. 10). When grouped by facies, facies 7 demonstrates the highest average CPI, and facies 4 contains the lowest average CPI (Fig. 6). Facies 7 shows the highest average ACL and lowest average *n*-C_{29}/*n*-C_{27}, but most facies display similar ACL and *n*-C_{29}/*n*-C_{27} values. Most facies also contain a similar total abundance of *n*-alkanes, with the highest average abundance in facies 3.

Two samples with representative *n*-alkane distributions were analysed for additional biomarkers (Supplementary table 2). Samples contained a range of C_{27}–C_{32} hopanes and C_{27}–C_{30} hopenes. The dominant compounds were 17β(H)-trisnorhopane (C_{27}), 17α,21β(H)-hopane (C30),17β,21β(H)-homohopane (C_{31}). Both samples were characterised by high ββ/(αβ+βα+ββ) ratios (0.69 to 1.00) and indicate low thermal maturity.

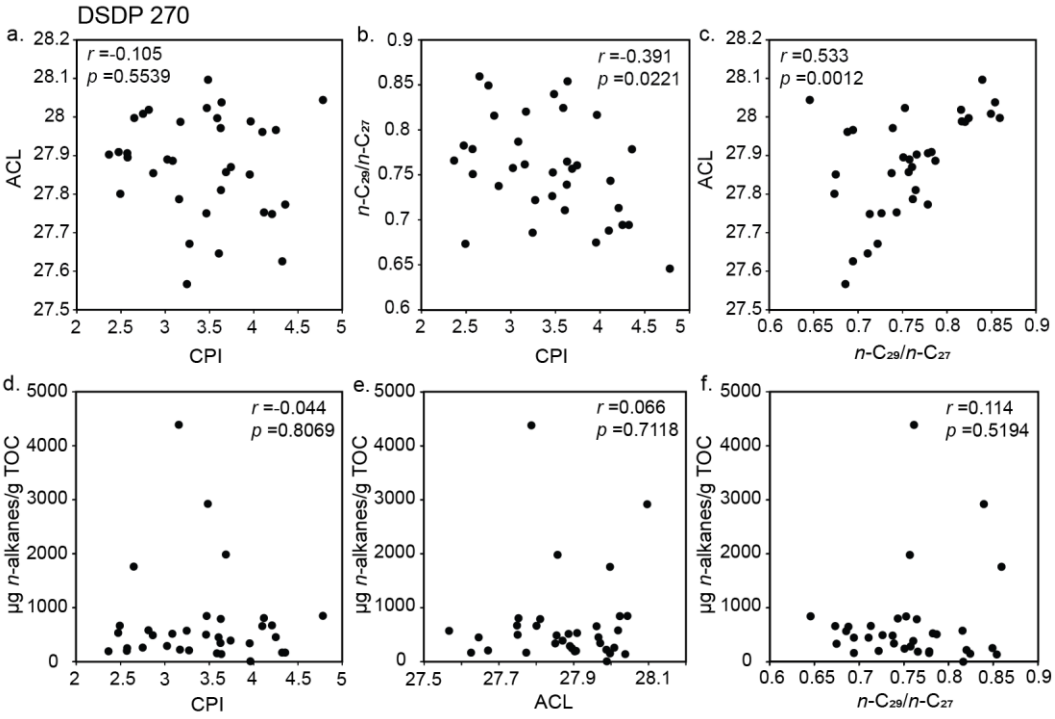

Fig. 10. Scatter plots of samples from DSDP 270; a) CPI and ACL; b) CPI and n-C_{29}/n-C_{27}; c) n-C_{29}/n-C_{27} and ACL; d) CPI and the total abundance of n-alkanes (µg n-alkanes/g TOC); e) ACL

and the total abundance of n-alkanes (μg n-alkanes/g TOC) and f) n-C_{29}/n-C_{27} and the total abundance of n-alkanes (μg n-alkanes/g TOC).

3.5 DSDP 274

Samples taken from above 115m had variable, or even absent, quantities of *n*-alkanes (Fig. 11). Samples usually contained significant UCMs, which typically dominated the signal, and *n*-alkanes did not display a common dominant *n*-alkane. Samples below 115m were usually bimodal in distribution, with a dominant *n*-alkane peak around *n*-C_{19}, *n*-C_{20} or *n*-C_{21}, underlain by a UCM, and another peak centred at *n*-C_{27}. CPI ranges from 0.6 to 3.0 (avg. 1.6), whilst ACL ranges from 25 to 31.0 (avg. 27.8). The ratio of *n*-C_{29} to *n*-C_{27} varies from 0.50 to 1.37 (avg. 0.80). The total abundance of *n*-alkanes averages 72.7 μg/gTOC, with a range of 2.7 μg/gTOC to 316.6 μg/gTOC (Supplementary table 1).

Pearson's correlation coefficients show the strongest correlations exist between CPI and *n*-C_{29}/*n*-C_{27} (r = 0.809, p < 0.0000), and ACL and *n*-C_{29}/*n*-C_{27} (r = 0.825, p < 0.0000) (Fig. 12). Weak correlations exist between the total abundance of *n*-alkanes and the other three variables considered; CPI, ACL and *n*-C_{29}/*n*-C_{27} (r = 0.350, p = 0.0461; r = 0.396, p = 0.0224; r = 0.389, p = 0.0338 respectively). Only one combination, CPI and ACL, does not indicate a statistically significant correlation, as ACL becomes much more variable at low CPIs. Facies 11 has significantly lower CPI and higher *n*-C_{29}/*n*-C_{27} than facies 10 (Fig. 6). ACL is much more variable in facies 11, and on average higher, while the total abundance of *n*-alkanes is on average lower than facies 10.

One sample from facies 11 was analysed for additional biomarkers (Supplementary table 2). The sample contained a range of thermally mature C_{27}–C_{35} hopanes. The dominant compounds were 17α,21β(H)-norhopane (C_{29}) and 17α,21β(H)-hopane (C30). This sample was characterised by low ββ/(αβ+βα+ββ) ratios (0), high C22S/C22R+C22S ratios (0.57) and moderate Ts/Ts+Tm ratio (0.31). Collectively, this indicates high thermal maturity.

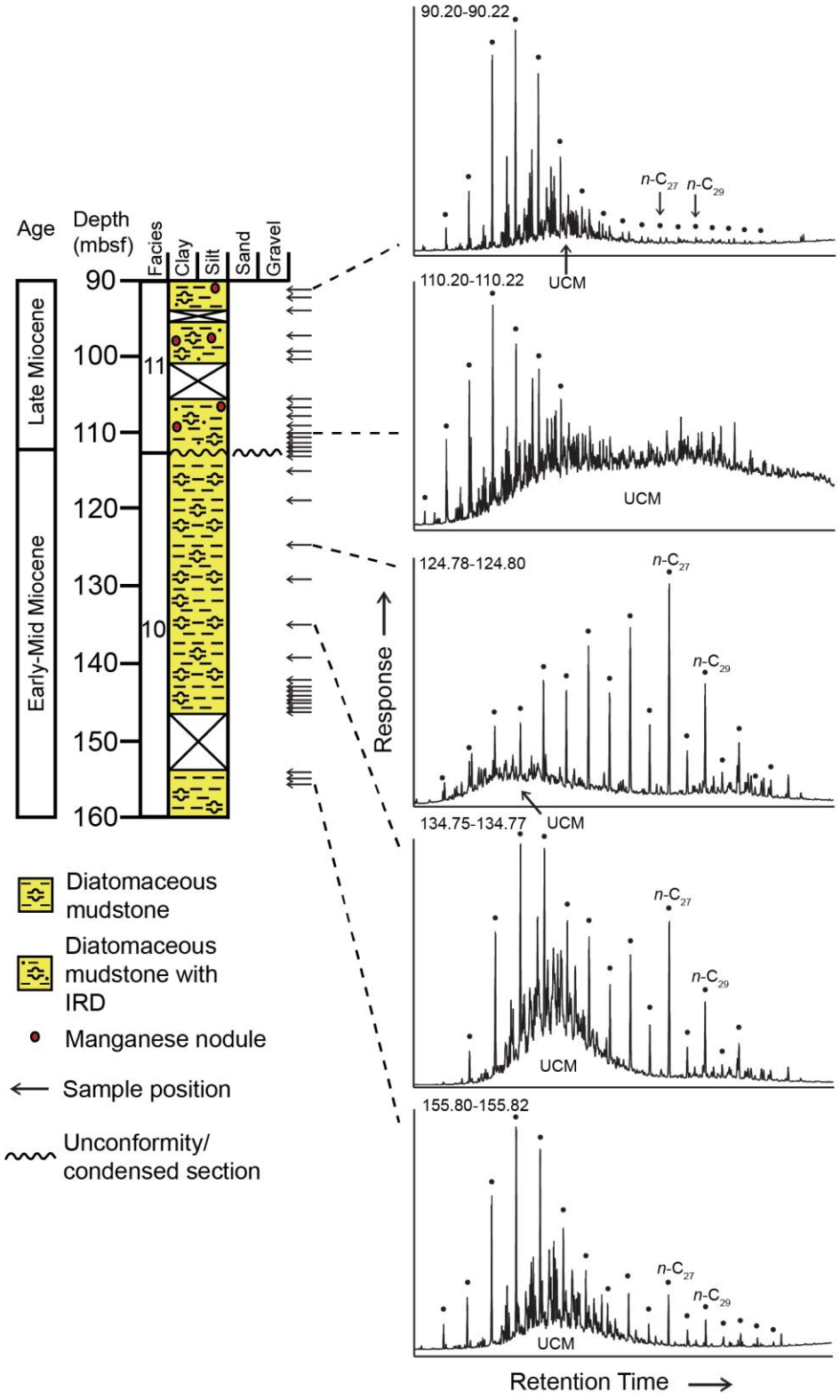

405

406 *Fig. 11. Stratigraphic column from DSDP 274 with the stratigraphic positions of*
407 *representative GC-FID-chromatograms of samples. Filled circles above peaks indicate n-alkanes,*
408 *with the n-C_{27} and n-C_{29} labelled. Facies are described in table 1. UCM: unresolved complex mixture.*

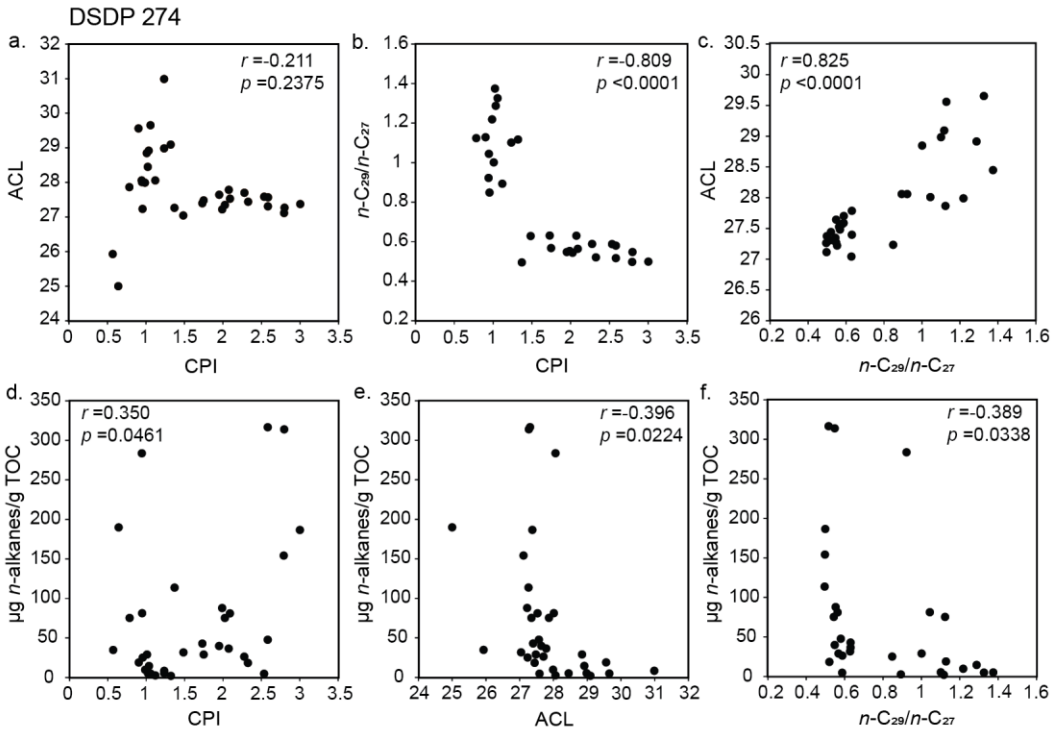

409

410 *Fig. 12. Scatter plots of samples from DSDP 274; a) CPI and ACL; b) CPI and n-C_{29}/n-C_{27};*
411 *c) n-C_{29}/n-C_{27} and ACL; d) CPI and the total abundance of n-alkanes (µg n-alkanes/g TOC); e) ACL*
412 *and the total abundance of n-alkanes (µg n-alkanes/g TOC) and f) n-C_{29}/n-C_{27} and the total*
413 *abundance of n-alkanes (µg n-alkanes/g TOC).*

414 **4 Discussion**

415 *4.1 Potential sources of lipid biomarkers in Cenozoic Antarctic sediments*

416 *4.1.1 Contemporaneous organic matter*

417 Plants and microorganisms living contemporaneously with the accumulation of sediment
418 would have been a major contributing source for *n*-alkanes and hopanes with ββ stereochemistry at
419 the sites studied. Macro- and microfossils from sediment cores, onland outcrops and glacial erratics
420 indicate that the Ross Sea region of Antarctica was vegetated until at least the Mid-Miocene Climate
421 Transition (MMCT) ~14 Ma (e.g. Kemp, 1975; Mildenhall, 1989; Askin, 2000; Askin and Raine,
422 2000; Lewis et al., 2008; Warny et al., 2009; Lewis and Ashworth, 2016). Paleocene and Early
423 Eocene sediment from cores offshore Wilkes Land indicate a highly diverse, near tropical flora
424 occupied coastal regions, with temperate rain forest inland and at higher elevations (Pross et al.,
425 2012). Following a prolonged period of global cooling, sediments from the Ross Sea region indicate
426 that by the Mid-Late Eocene, vegetation was largely represented by a less diverse, cool, temperate
427 flora dominated by *Nothofagus*-podocarpaceous conifer-proteaceae (Askin, 2000; Francis, 2000; Pole
428 et al., 2000).

The Oligocene and early Miocene was marked by declining vegetation diversity and the development of a sparse, shrubby tundra, dominated by stunted *Nothofagus* (Kemp, 1975; Kemp and Barrett, 1975; Askin and Raine, 2000; Prebble et al., 2006a). The Mid-Miocene Climate Optimum (MMCO) (~17-15 Ma), saw an increase in the abundance of pollen transported offshore indicating a proliferation of woody vegetation and a possible return to more tree-like forms (Warny et al., 2009; Feakins et al., 2012). This short-lived warming was followed by the MMCT, a major cooling step in the Cenozoic (Shackleton and Kennett, 1975; Flower and Kennett, 1994; Lewis et al. 2007). The vegetation history of Antarctica following the MMCT has been debated, with different schools of thought suggesting that demise of higher plants occurred either at the MMCT (Sugden et al., 1993; Marchant et al., 1996; Lewis et al., 2008) or the Pliocene (Harwood et al. 1983; Webb et al. 1984; Fielding et al., 2012). The Pliocene ages are controversial and rely on sparse diatoms present in tills of the Meyer Desert Formation, preserved in the upper Beardmore Glacier (Barrett, 2013).

4.1.2 Reworked lipid biomarkers from older sediments

Lipid biomarkers could also be sourced from the erosion and redeposition of older sediments. Two main sources are considered here; reworked Cenozoic *n*-alkanes, and reworked Permian-Jurassic biomarkers sourced from the Beacon Super Group and Ferrar Group. The presence of Cretaceous dinoflagellate cysts in samples of the McMurdo erratics suggests the possibility for a contribution from rocks of this age now either eroded or buried, but as these occurrences are extremely rare this potential contribution is considered very minor (Askin, 2000). Surface sediment from the Eastern Ross Sea does contain a significant component of Late Cretaceous palynomorphs, but the location of DSDP Site 270 in the central Ross Sea does not (Truswell and Drewry, 1984). Oligocene/Late Miocene sediments in this core are also barren of pollen from this time period (Kemp, 1975; Duncan, 2017).

Microfossil work on Oligocene and Miocene sediments in continental margin drillcores frequently indicate the presence of older Cenozoic microfossils, likely eroded from older sedimentary basin infill. In particular, Eocene aged dinoflagellate cysts of the 'Transantarctic flora' are used to infer reworking of Eocene material into younger sediments (e.g. Kemp, 1975; Askin and Raine, 2000; Prebble et al., 2006a). Limited burial of Cenozoic sediments means that Paleogene forms reworked into younger sediments are still light in colour and display similar autofluorescence (e.g. Askin and Raine, 2000; Prebble et al., 2006a). Here, *n*-alkanes extracted from the fossiliferous McMurdo erratics serve as an indication of typical Mid-Late Eocene distributions of these compounds (Section 4.2.1).

The Beacon Supergroup extends throughout the TAM and is a key source of sediment to the sedimentary basins of the Ross Sea (e.g. Talarico et al., 2000; Smellie, 2001; Sandroni and Talarico, 2004; Sandroni and Talarico, 2011). Many of the fossil assemblages from the Beacon Supergroup come from widespread Permian and Triassic sediments, and indicate a cool, humid Mid-Late Permian

climate with vegetation dominated by *Glossopteris* and *Gangamopteris* (Cúneo et al., 1993; Francis et al., 1994; Collinson, 1997). By the Mid-Triassic, a more diverse flora dominated by *Dicroidium* indicates a shift to warmer 'greenhouse' conditions (Collinson, 1997; Cúneo et al., 2003). The Beacon Supergroup outcropping in the TAM has undergone widespread intrusion and thermal alteration, with altered palynomorphs in continental margin cores likely reflecting a TAM source, whilst less altered specimens must have been transported from less extensively intruded sediments cratonwards of the TAM (Askin, 1998; Askin and Raine, 2000). Fossiliferous sedimentary interbeds of the Jurassic Ferrar group are also known to contribute reworked palynomorphs to offshore sediments, albeit with much rarer occurrences than those sourced from the Beacon Supergroup (Askin and Raine, 2000). *n*-Alkanes have previously been analysed from Beacon sediments, silicified wood and coal at the Allan Hills and Ferrar Group sediments from Carapace Nunatak in Southern Victoria Land (Matsumoto et al., 1986). *n*-Alkanes ranging from *n*-C_{12} to *n*-C_{30} displayed a CPI varying from 0.91-1.4. Short chain *n*-alkanes (< *n*-C_{20}) were typically more abundant than long chain lengths (Matsumoto et al., 1986). A chromatogram from Matsumoto et al. (1986) indicates that UCMs are also present in these samples, centred at *n*-C_{18} and *n*-C_{19}. Hopanes in these Beacon sediments were typically dominated by αβ and βα configurations indicating maturation of the sediments and alteration of hopanes from their biologically synthesized precursors (Matsumoto et al., 1987). Variable thermal maturation of the Beacon sediments in this region is suggested by two samples containing small quantities of ββ hopanes (Matsumoto et al., 1987)

Distributions of *n*-alkanes, kerogen and palynomorphs in surface and Quaternary sediments from the Ross Sea, and soils from the Dry Valleys, suggest the potential for recycling of *n*-alkanes from both Cenozoic and pre-Cenozoic sources is occurring via modern depositional processes. In the Ross Sea, *n*-Alkanes appear in low abundances with short chained *n*-alkanes attributed to a mixture of primary and recycled material derived from marine organisms, while long chained *n*-alkanes are suggested to be higher plant material either from long-range aeolian transport or reworked from pre-Quaternary sediments (Kvenvolden et al., 1987; Venkatesan, 1988). A recycled source for *n*-alkanes is supported by the presence of hopanes of variable maturities (ββ, βα and αβ), and kerogen and pollen extensively reworked from Paleogene or pre Cenozoic sediment (Sackett et al., 1974; Truswell and Drewry, 1984, Kvenvolden et al., 1987). The most abundant *n*-alkanes in soils from the Dry Valleys are usually *n*-C_{23}, *n*-C_{25}, or *n*-C_{27} (Matsumoto et al., 1990a; Matsumoto et al., 2010; Hart et al., 2011). *n*-Alkanes are attributed to a mixed source input, predominantly derived from endolithic microorganisms and glacially eroded ancient plant and microorganism debris, sourced from earlier Cenozoic sediments and the Beacon Sandstone (Matsumoto et al., 1990a; Matsumoto et al., 2010). This is supported by the presence of mature (βα and αβ) isomers of hopanes, likely sourced from Beacon sediments (Matsumoto et al., 1990b) Aeolian transport as a main source for the *n*-alkanes in these samples is considered unlikely, as aerosol samples near Antarctica record *n*-alkane distributions

with high ACLs and a dominant *n*-C_{31}, potentially as a result of large scale meridional air mass circulation transporting *n*-alkanes from the tropics to high latitudes (Bendle et al., 2007).

4.1.3 In situ degradation of n-alkanes

In Antarctica and the Sub-Antarctic, hydrocarbon contamination experiments indicate that hydrocarbon degrading microbes are present in soils (Aislabie et al., 1998; Bej et al., 2000; Coulon et al., 2005). Longer chain length *n*-alkanes were found to be more resistant to microbial degradation, and rates of degradation increase with increasing temperature (Coulon et al., 2005). *n*-Alkane distributions in the studied samples are not considered the result of *in situ* thermal maturation, or migration of hydrocarbons into the sediments. The sediment sampled in this study comes from near surface sediment in the case of Mt Boreas, or drill cores where the deepest samples come from 385 mbsf in DSDP 270. None of the studied cores contained hydrocarbon residues, and heat flow measurements from CRP-2/2A and other cores in the region (CRP 3, ANDRILL 1B, ANDRILL 2A) range from 24-76.7 °C/km (Bücker et al., 2000; Bücker et al., 2001; Morin et al., 2010; Schröder et al., 2011). Basin modelling from the central and western Ross Sea shows that while the generation of hydrocarbons is possible in the deeply buried sediments of the basins, expulsion and migration of hydrocarbons from potential source rocks is very unlikely (Strogen and Bland, 2011).

4.2 n-Alkane distributions across sample sites

4.2.1 McMurdo erratics

The McMurdo erratics provide examples of mid-late Eocene *n*-alkane distributions, when Antarctic vegetation was more diverse than in the Oligocene and Miocene, and the climate was warmer and wetter (Askin, 2000; Francis, 2000; Pole et al., 2000). All of the samples except for MTD95 contain a terrestrial palynomorph assemblage, with E215 and E219 also including leaves and in E219, wood macrofossils (Harwood and Levy, 2000). However, these erratics do also contain a minor component of reworked material sourced from the Beacon Supergroup (Askin, 2000). Despite this, the occurrence of macro-fossils and dominantly Eocene-aged assemblages of palynomorphs suggest that the *n*-alkanes in these samples are principally from contemporaneously-sourced organic matter. The key difference in the *n*-alkane distributions of the McMurdo erratics compared to Oligocene and Miocene samples from the other studied sites is the prominence of the *n*-C_{29} as opposed to the *n*-C_{27} (Supplementary table 1, Fig.3). We suggest the shift from a dominant *n*-C_{29} to *n*-C_{27} in the Ross Sea region is due to a combination of climate cooling as the Antarctic ice sheets developed, and a shift in plant community to a flora dominated by a low diversity tundra of *Nothofagus, podocarpidites* and bryophytes (Askin, 2000; Askin and Raine, 2000; Prebble et al., 2006a; Lewis et al., 2008).

4.2.2 Mt Boreas

The presence of macro and microfossils of bryophytes at Mt Boreas is represented by the prominence of *n*-C_{23} and *n*-C_{25} in the *n*-alkane distributions from this site (Fig. 4) (Lewis et al., 2008). The *n*-C_{27} homolog is also particularly abundant and is likely sourced from shrubs and trees such as *Nothofagidites lachlaniae* in the lake catchment (Lewis et al., 2008). A correlation between increasing *n*-C_{29} and decreasing CPI could be the result of either: 1) microbial degradation lowering CPI and preferentially degrading the shorter chain *n*-C_{27}; or 2) incorporation of recycled material, likely from weathered, thermally-degraded Beacon Supergroup, and older Cenozoic sediments in the catchment. This is supported by the presence of thermally matured hopanes in sample ALS-05 21O, which is from the base of the lacustrine section, just above a glacial till containing clasts of Beacon Supergroup (Lewis et al., 2008). Other samples in which hopanes were investigated were dominated by ββ hopanes, supporting an interpretation that much of the biomarkers in the rest of the lacustrine sediments are contemporaneously sourced. Lacustrine depositional environments (Facies 1) have higher average CPIs and lower average *n*-C_{29}/*n*-C_{27} values than fluvial samples (Facies 2) (Fig. 6). Fluvial environments can be erosive settings as coarser sediments require greater water velocity for suspension and movement (Miller et al., 1977), suggesting a fluvially influenced environment is more likely to rework *n*-alkanes. In the lacustrine setting, high CPI, low ACL and *n*-C_{29}/*n*-C_{27} in particular occur directly below, and almost directly above the moss peat (Fig. 4). *n*-alkane distributions are likely sampling the aquatic plants and mosses deposited during a shallow water phase of the lake. Samples from beds representing a deeper water phase of the lake (Lewis et al., 2008) are marked by a similar average CPI and *n*-C_{29}/*n*-C_{27} as the laminated silts, but a higher ACL, reflecting an increased input of emergent and terrestrial plant matter from the surrounding catchment.

4.2.3 CRP 2/2A

In CRP 2/2A, *n*-alkane distributions typically show the *n*-C_{27} as the dominant homolog, although *n*-C_{23}, *n*-C_{25} and *n*-C_{29} were also commonly abundant. The prominence of these *n*-alkane homologs is in line with palynomorph evidence which suggests input from trees, shrubs and bryophytes (Prebble et al., 2006a). Fluctuating abundances of reworked palynomorphs (thermally altered, poorly preserved or of a known older range) often coincide with larger abundances of Eocene Transantarctic flora dinoflagellates (Prebble et al., 2006a). This indicates reworked samples were sourced from both Permian/Triassic Beacon sediments and earlier Cenozoic sediments. The correlations between low CPI, and high ACL and *n*-C_{29}/*n*-C_{27} (Fig. 8) can be explained by a mixed source input of *n*-alkanes, from contemporaneous material, early Cenozoic sediments, and both altered and unaltered areas of the Beacon Supergroup. This is supported by the presence of both biologically synthesized and thermally matured hopane configurations. While a contribution from more recent recycled material (i.e Early Oligocene *n*-alkanes) cannot be ruled out, Prebble et al.

(2006b) found little evidence for reworking between Early and Late Oligocene sequences. UCMs in these samples typically underlie the lower chain lengths, and may be the result of post-depositional microbial alteration, or could be inherited from the Beacon Supergroup (Matsumoto et al., 1986). Facies groupings reflect depositional environments which are predominantly influenced by the proximity of glaciers near the site. More ice-distal, marine facies (7 and 8) have on average high CPIs, low ACL and low *n*-C_{29}/*n*-C_{27} (Fig. 6), while samples from ice-proximal or subglacial settings tend to show the opposite trends. This suggests that low-energy, more ice-distal marine environments are more likely to contain well-preserved *n*-alkane distributions reflecting contemporaneously sourced *n*-alkanes, whilst more ice-proximal and subglacial environments have a higher likelihood of containing reworked *n*-alkanes.

4.2.4 DSDP 270

n-Alkane distributions from DSDP 270 are typically bi-modal suggesting two primary sources for *n*-alkanes in this drill core (Fig. 9). Algae and bacteria the likely source for the shorter chain lengths, with terrestrial higher plants contributing to longer chain lengths (section 2.5). The presence of a contemporaneous pollen assemblage with almost no reworked contribution indicates the long chained *n*-alkanes predominantly reflect contemporary onshore vegetation. This is shown in the CPI values that vary less than the other sites sampled and all sit above 2.4 (Fig. 6), and the predominance of hopanes in ββ configurations. Facies representing more ice-proximal settings (facies 3 and 4) show the lowest average CPIs suggesting that these settings are likely to contain more degraded *n*-alkane distributions, whether as the result of post-depositional processes or some sediment recycling due to glacial erosion and redeposition (Fig. 6).

4.2.5 DSDP 274

n-Alkane distributions in DSDP 274 are separated into two distinct groups, above and below an unconformity/condensed section at 113.6 mbsf (Figs. 6 and 11). Samples taken from below 113.6 mbsf show bi-modal distributions in chromatograms suggesting a mixed contribution from both algae and bacteria, and terrestrial plants. Other than the uppermost 2 samples from this section of the core, all samples are considered to be part of facies 10, which was deposited with a high terrigenous and biogenic sedimentation rate, under a regime of weak bottom currents (Fig. 2) (Frakes, 1975; Whittaker and Müller, 2006). Reworked palynomorphs are present in this section (Kemp, 1975), which, coupled with variable CPI and UCMs suggest that some contribution of reworked *n*-alkanes is likely. However, the generally high CPI, dominance of the *n*-C_{27} and lack of variation in ACL and *n*-C_{29}/*n*-C_{27} suggests that much of the *n*-alkanes present reflect comparatively more contemporaneous input than the overlying interval, or at least material recycled from the Oligocene or younger.

Above the unconformity or condensed section at 113.6 mbsf, the sedimentation rate slows and manganese nodules provide evidence for winnowing by a strong bottom current regime. This interval is also associated with an increase in coarse sediment which could result from ice rafting (Frakes, 1975; Whittaker and Müller, 2006) or winnowing of the fine fraction due to intensification of bottom currents. These sediments date to the Late Miocene, and Antarctic glacial expansion at this time could explain the increase in ice rafting or bottom water current intensity (McKay et al., 2009; Herbert et al., 2016). Sediments from this part of the core are also include and post-date the MMCT when it has been debated that higher plants became extinct on Antarctica (Sugden et al., 1993; Marchant et al., 1996; Lewis et al., 2008). This indicates that *n*-alkanes from this section of the core may predominantly be derived from older sediments, an interpretation supported by a hopane distribution dominated by thermally matured configurations. Low CPIs, high n-C_{29}/n-C_{27}, often large and dominant UCMs and low sedimentation rates suggest that *n*-alkanes in these samples have also been extensively degraded, likely by microbial activity as sediments are winnowed and reworked in the surface layers of the seabed.

5. Synthesis

n-Alkane distributions in Eocene to Miocene sediments from the Ross Sea region vary with age and sample site. Between the Eocene and Oligocene, the dominant chain length recorded in sediments changes from n-C_{29} to n-C_{27}, concomitant with a significant climate cooling and a shift in plant community (section 4.2.1). The dominance of the n-C_{27} in sediments sourced from wide catchments incorporating a cool, low diversity vegetation dominated by *Nothofagus* is in contrast to lower latitudes where n-C_{29} and n-C_{31} are often more abundant (e.g. Poynter et al., 1989; Kawamura et al., 2003; Sachse et al., 2006; Bendle et al., 2007). At least one modern species of *Nothofagus* (*N. menziesii*) from New Zealand has been shown to produce n-C_{27} as its dominant *n*-alkane (Burrington, 2015), while other species in New Zealand and South America are typically dominated by n-C_{29} and n-C_{31} (Schellekens et al., 2009; Schellekens et al., 2011; Burrington, 2015). The high abundance of n-C_{27} in samples from Mt Boreas also containing abundant pollen from *N. lachlaniae* suggest that this species was likely producing large proportions of this *n*-alkane. The prominence of the n-C_{27} across the Oligocene and Miocene sites of this study likely reflects both a climate adaption by plants growing in the Antarctic tundra to cold temperatures, and the abundance of *Nothofagus* in the catchments.

While the Oligocene and Miocene vegetation of Antarctica was a main source of *n*-alkanes to the sample sites, reworked *n*-alkanes and hopanes from early and pre-Cenozoic sediments were also evident. In particular, variables that often characterised samples with more reworked material were low CPI values, but higher ACLs and n-C_{29}/n-C_{27} ratios. In a sample containing material solely from reworked thermally altered sections of the Beacon Supergroup, a low CPI, ACL and n-C_{29}/n-C_{27}

would be expected (Matsumoto et al., 1986). The association of low CPIs with high ACL and *n*-C_{29}/*n*-C_{27} therefore suggests that reworked samples likely contain a mixture of *n*-alkanes derived from thermally matured Beacon sediments, coupled with material from early Cenozoic and less altered pre-Cenozoic sediments containing a higher abundance of longer chained *n*-alkanes such as *n*-C_{29} and *n*-C_{31}. In some instances, this distribution could also result from microbial degradation, which could lower CPI, whilst also preferentially scavenging shorter chain lengths.

Sediments deposited by glacio-fluvial, ice-proximal glaciomarine and subglacial processes are more likely to contain reworked *n*-alkane distributions than those from lacustrine or ice-distal marine environments, although careful site specific consideration of sediment provenance must be undertaken, regardless of relative proximity to glaciers or rivers. Prior to the MMCT, glaciers throughout the TAM, and likely the exposed areas of the Ross Sea, were warm-based (Marchant and Denton, 1996; Lewis et al., 2007). This regime would have favoured high rates of glacial erosion of underlying strata, resulting in rapid remobilisation, deposition and burial of sediment in glacial proximal regions (Sugden and Denton, 2004; Powell et al. 2000). These processes likely led to the deposition of greater proportions of reworked *n*-alkanes in ice-proximal environments. Although ice-distal settings also record glaciomarine processes and may be subject to reworking, they are likely a more integrated record of aeolian and glacio-fluvial sediment transport offshore. However, as Antarctica became progressively more arid during the Late Miocene and Pliocene, it is feasible that offshore transport of contemporaneous *n*-alkanes via glacio-fluvial action reduced, and thus the relative input of reworked *n*-alkanes became more prominent (e.g. at DSDP 274).

The varying contribution of contemporaneous and reworked biomarkers across sediments sourced from different depositional environments, catchments and ages emphasizes how caution must be exercised when applying biomarker-based paleoclimate proxies in glacially-influenced settings (e.g. *n*-alkane $\delta^{13}C$ and $\delta^{2}H$). In particular, several aspects should be considered when determining if an *n*-alkane distribution is a contemporaneously-sourced organic matter signature. These include the values and variation of factors such as CPI and ACL, maturation indices of other biomarkers such as hopanes, whether the catchment and depositional setting of a site is more likely to accumulate and preserve a contemporary distribution, and assemblages of other fossil material such as palynomorphs. When constructing timeseries of biomarker assemblages, it is also important to consider other aspects of the depositional environment in the Ross Sea. The coastal setting of the Ross Sea could be influenced by pulses of reworked material, given the potential for point source glacial meltwater discharge, and large-scale meltwater discharge events (i.e. Powell and Domack, 2002; Lewis et al., 2006), which may focus erosion to a certain lithological source. Input of reworked material via episodic, erosive hydrological events in Paleocene-Eocene Thermal Maximum sediments from Tanzania has been invoked to explain the highly variable *n*-alkane $\delta^{13}C$ values in these sediments (Carmichael et al., 2017). Glacially-influenced environments have a high potential to erode and

almost instantaneously redeposit older biomarkers and pollen offshore in concentrated numbers, and indeed biomarker distributions could be used as a potential tool to identify such reworking events.

6 Conclusions

n-Alkane and hopanoid distributions have been characterised in Eocene to Miocene sediments from a range of depositional environments in the Ross Sea region of Antarctica. Between the Late Eocene and the Oligocene, a shift in *n*-alkane dominant chain length is observed from *n*-C_{29} to *n*-C_{27}. This is inferred to be a result of both a shift in plant community, as well as a response to significant climate cooling. Biomarker distributions in Oligocene and Miocene samples varyingly display a contribution from both contemporaneous and reworked sources. *n*-Alkane distributions typical of a reworked sample were a low CPI, and high ACL and *n*-C_{29}/*n*-C_{27} values. Reworked samples likely reflect a mixed contribution from thermally altered and less thermally altered regions of the Mesozoic Beacon Super Group, coupled with material sourced from earlier Cenozoic sediments. Microbial degradation during transport and post-deposition may also contribute to these distributions. Samples dominated by contemporaneously-sourced organic matter display a higher CPI, and lower ACL and *n*-C_{29}/*n*-C_{27} values. These *n*-alkanes were sourced from the sparse, cold tundra which existed during this time. Fluvial environments onshore, and subglacial and ice-proximal environments offshore were more likely to contain reworked *n*-alkanes. Lacustrine environments onshore, and ice-distal environments offshore, were more likely to contain contemporary *n*-alkanes. These findings indicate the possibility of reworking should be taken into account when biomarkers are used for paleoclimate studies in ice-marginal environments.

7 Acknowledgments

The authors are grateful for access to samples from the IODP core repository at Texas A&M University for DSDP Sites 270 and 274. This study was funded via an Antarctica New Zealand Sir Robin Irvine PhD Scholarship and Scientific Committee of Antarctic Research Fellowship awarded to Bella Duncan, with additional funding from a Royal Society of New Zealand Rutherford Discovery Fellowship awarded to Rob McKay (RDF-13-VUW-003) and New Zealand Ministry of Business Innovation and Employment Contract C05X1001. Field activities were supported by Antarctica New Zealand. The authors are grateful for support from IODP and support in kind from the University of Birmingham. The authors thank two anonymous reviewers for their constructive comments.

Data Availability

Data associated with this study can be found in the supplementary tables.

References

Aislabie, J., McLeod, M., Fraser, R., 1998. Potential for biodegradation of hydrocarbons in soil from the Ross Dependency, Antarctica. Applied Microbiology and Biotechnology 49, 210-214.

Allibone, A.H., Cox, S.C., Graham, I.J., Smillie, R.W., Johnstone, R.D., Ellery, S.G., Palmer, K., 1993. Granitoids of the Dry Valleys area, southern Victoria Land, Antarctica: plutons, field relationships, and isotopic dating. New Zealand journal of geology and geophysics 36, 281-297.

Allibone, A.H., Cox, S.C., Smillie, R.W., 1993. Granitoids of the Dry Valleys area, southern Victoria Land: geochemistry and evolution along the early Paleozoic Antarctic Craton margin. New Zealand journal of geology and geophysics 36, 299-316.

Askin, R.A., 1998. Palynological investigations of Mount Feather Sirius Group samples: recycled Triassic assemblages, In: Wilson, G.S., Barron, J. (Eds.), Mount Feather Sirius Group Core Workshop and Collaborative Sample Analysis. Byrd Polar Research Center Report No. 14. Byrd Polar Research Center, The Ohio State University, Columbus, Ohio, pp. 59-65.

Askin, R.A., 2000. Spores and pollen from the McMurdo Sound erratics, Antarctica. In: Stilwel, J.D., Feldman, R.M. (Eds.), Paleobiology and Paleoenvironments of Eocene Rocks: McMurdo Sound, East Antarctica. American Geophysical Union, Washington, D.C., pp. 161-181.

Askin, R.A., Raine, J.I., 2000. Oligocene and Early Miocene terrestrial palynology of the Cape Roberts Drillhole CRP-2/2A, Victoria Land Basin, Antarctica. Terra Antarctica 7, 493-501.

Barrett, P.J., 1981. History of the Ross Sea region during the deposition of the Beacon Supergroup 400-180 million years ago. Journal of the Royal Society of New Zealand 11, 447-458.

Barrett, P.J., Elliot, D.H., Lindsay, J.F., 1986. The Beacon Supergroup (Devonian- Triassic) and Ferrar Group (Jurrasic) in the Beardmore Glacier Area, Antarctica. In: Turner, M.D., Splettstoesser J.E. (Eds.), Geology of the central Transantarctic Mountains. American Geophysical Union, Washington, D.C., pp. 339-428.

Barrett, P.J. (Ed.). 1989. Antarctic Cenozoic history from the CIROS-1 drillhole, McMurdo Sound. DSIR Publishing, Wellington, New Zealand.

Barrett, P.J., 2013. Resolving views on Antarctic Neogene glacial history–the Sirius debate. Earth and Environmental Science Transactions of the Royal Society of Edinburgh 104, 31-53.

Bej, A.K., Saul, D., Aislabie, J., 2000. Cold-tolerant alkane-degrading Rhodococcus species from Antarctica. Polar Biology 23, 100-105.

Bendle, J., Kawamura, K., Yamazaki, K., Niwai, T., 2007. Latitudinal distribution of terrestrial lipid biomarkers and n-alkane compound-specific stable carbon isotope ratios in the atmosphere over the western Pacific and Southern Ocean. Geochimica et Cosmochimica Acta 71(24), 5934-5955.

Bijl, P.K., Bendle, J.A., Bohaty, S.M., Pross, J., Schouten, S., Tauxe, L. Stickley, C.E., McKay, R.M., Röhl, U., Olney, M., Sluijs, A., Escutia, C., Brinkhuis, H., Expedition 318 Scientists, 2013.

739 Eocene cooling linked to early flow across the Tasmanian Gateway. Proceedings of the
740 National Academy of Sciences 110, 9645-9650.
741 Bray, E.E., Evans, E.D., 1961. Distribution of n-paraffins as a clue to recognition of source
742 beds. Geochimica et Cosmochimica Acta 22, 2-15.
743 Bücker, C.J., Wonik, T., Jarrard, R., 2000. The temperature and salinity profile in CRP-2/2A, Victoria
744 Land Basin, Antarctica. Terra Antarctica 7, 255-259.
745 Bücker, C., Jarrard, R.D., Wonik, T., 2001. Downhole temperature, radiogenic heat production, and
746 heat flow from the CRP-3 drillhole, Victoria Land Basin, Antarctica. Terra Antarctica 8, 151-
747 160.
748 Burrington, P., 2015. How to be a Prehistoric Weatherman: Using n-alkanes as a Proxy for Holocene
749 Climate and Hydrology, Southwest South Island, New Zealand (Unpublished Masters Thesis).
750 University of Otago, New Zealand.
751 Bush, R.T., McInerney, F.A., 2013. Leaf wax n-alkane distributions in and across modern plants:
752 implications for paleoecology and chemotaxonomy. Geochimica et Cosmochimica Acta 117,
753 161-179.
754 Bush, R.T., McInerney, F.A., 2015. Influence of temperature and C_4 abundance on n-alkane chain
755 length distributions across the central USA. Organic Geochemistry 79, 65-73.
756 Calvo, E., Pelejero, C., Logan, G.A., De Deckker, P., 2004. Dust-induced changes in phytoplankton
757 composition in the Tasman Sea during the last four glacial cycles. Paleoceanography 19.
758 Cape Roberts Science Team, 1999. Studies from the Cape Roberts Project, Ross Sea Antarctica,
759 Initial report on CRP-2/2A. Terra Antarctica 6(1), 1-173.
760 Carmichael, M. J., Inglis, G. N., Badger, M. P., Naafs, B. D. A., Behrooz, L., Remmelzwaal, S.,
761 Monteiro, F. M., Rohrssen, M., Farnsworth, A., Buss, H. L., Dickson, A. J., Valdes, P. J., Lunt,
762 D. J., Pancost, R. D., 2017. Hydrological and associated biogeochemical consequences of rapid
763 global warming during the Paleocene-Eocene Thermal Maximum. Global and Planetary
764 Change 157, 114-138.
765 Clark Jr, R.C., Blumer, M., 1967. Distribution of n-paraffins in marine organisms and
766 sediment. Limnology and Oceanography 12, 79-87.
767 Collinson, J.W., 1997. Paleoclimate of Permo-Triassic Antarctica. International Symposium on
768 Antarctic Earth Sciences 7, 1029-1034.
769 Cooper, A.K., Davey, F.J., Behrendt, J.C., 1987. Seismic stratigraphy and structure of the Victoria
770 Land basin, western Ross Sea, Antarctica. In: Cooper, A.K., Davey, F.J. (Eds.), The Antarctic
771 Continental Margin: Geology and Geophysics of the Western Ross Sea. Circumpacific Council
772 for Energy and Mineral Resources, Houston, T.X., pp. 27-65.
773 Coulon, F., Pelletier, E., Gourhant, L., Delille, D., 2005. Effects of nutrient and temperature on
774 degradation of petroleum hydrocarbons in contaminated sub-Antarctic soil. Chemosphere 58,
775 1439-1448.

776 Cranwell, P.A., Eglinton, G., Robinson, N., 1987. Lipids of aquatic organisms as potential
777 contributors to lacustrine sediments—II. Organic Geochemistry 11, 513-527.
778 Cúneo, N.R., Isbell, J., Taylor, E.L., Taylor, T.N., 1993. The Glossopteris flora from Antarctica:
779 taphonomy and paleoecology. Comptes Rendus XII ICC-P 2, 13-40.
780 Cúneo, N.R., Taylor, E.L., Taylor, T.N., Krings, M., 2003. In situ fossil forest from the upper
781 Fremouw Formation (Triassic) of Antarctica: paleoenvironmental setting and paleoclimate
782 analysis. Palaeogeography, Palaeoclimatology, Palaeoecology 197, 239-261.
783 Decesari, R.C., Sorlien, C.C., Luyendyk, B.P., Wilson, D.S., Bartek, L.R., Diebold, J., Hopkins, S.E.,
784 2007. Regional seismic stratigraphic correlations of the Ross Sea: implications for the tectonic
785 history of the West Antarctic Rift System. In: Cooper, A.K., Raymond, C.R., 10th ISAES
786 Editorial Team (Eds.), Antarctica: A Keystone in a Changing World- Online Proceedings of the
787 10th ISAES, 2007-1047, USGS Open-File Report, Short Research Paper 052, 4p.
788 De Santis, L., Anderson, J.B., Brancolini, G., Zayatz, I., 1995. Seismic record of late Oligocene
789 through Miocene glaciation on the central and eastern continental shelf of the Ross Sea. In:
790 Cooper, A.K., Barker, P.F., Brancolini, G. (Eds.), Geology and Seismic Stratigraphy of the
791 Antarctic Margin. American Geophysical Union, Washington, D.C., pp. 235-260.
792 Dodd, R.S., Rafii, Z.A., Power, A.B., 1998. Ecotypic adaptation in Austrocedrus chilensis in cuticular
793 hydrocarbon composition. New Phytologist 138, 699-708.
794 Dodd, R.S., Afzal-Rafii, Z., 2000. Habitat-related adaptive properties of plant cuticular
795 lipids. Evolution 54, 1438-1444.
796 Duncan, B.J., 2017. Cenozoic Antarctic climate evolution based on molecular and isotopic biomarker
797 reconstructions from geological archives in the Ross Sea region (Unpublished PhD Thesis).
798 Victoria University of Wellington, New Zealand.
799 Eglinton, G., Hamilton, R.J., 1963. The distribution of alkanes. Chemical plant taxonomy 187, 217.
800 Farrimond, P., Taylor, A., TelnÆs, N., 1998. Biomarker maturity parameters: the role of generation
801 and thermal degradation. Organic Geochemistry 29, 1181-1197.
802 Feakins, S.J., Warny, S., Lee, J.E., 2012. Hydrologic cycling over Antarctica during the middle
803 Miocene warming. Nature Geoscience 5, 557-560.
804 Feakins, S.J., Warny, S., DeConto, R.M., 2014. Snapshot of cooling and drying before onset of
805 Antarctic Glaciation. Earth and Planetary Science Letters 404, 154-166.
806 Feakins, S.J., Peters, T., Wu, M.S., Shenkin, A., Salinas, N., Girardin, C.A., Bentley, L.P., Blonder,
807 B., Enquist, B.J., Martin, R.E., Asner, G.P., Asner, G.P., 2016. Production of leaf wax n-
808 alkanes across a tropical forest elevation transect. Organic Geochemistry 100, 89-100.
809 Ficken, K.J., Li, B., Swain, D.L., Eglinton, G., 2000. An n-alkane proxy for the sedimentary input of
810 submerged/floating freshwater aquatic macrophytes. Organic Geochemistry 31, 745-749.
811 Fielding, C.R., Naish, T.R., Woolfe, K., Lavelle, M., 2000. Facies analysis and sequence stratigraphy
812 of CRP-2/2A, Victoria Land Basin, Antarctica. Terra Antarctica 7, 323-338.

Fielding, C.R., Henrys, S.A., Wilson, T.J., 2006. Rift history of the western Victoria Land Basin: a new perspective based on integration of cores with seismic reflection data. In D.K. Fütterer, D. Damaske, G. Kleinschmidt, H. Miller & F. Tessensohn (Eds.), Antarctica (pp. 309-318). Berlin Heidelberg: Springer.

Fielding, C.R., Harwood, D.M., Winter, D.M., Francis, J.E., 2012. Neogene stratigraphy of Taylor Valley, Transantarctic Mountains, Antarctica: evidence for climate dynamism and a vegetated early Pliocene coastline of McMurdo Sound. Global and Planetary Change 96-97, 97-104.

Fitzgerald, P.G., 1994. Thermochronologic constraints on post-Paleozoic tectonic evolution of the central Transantarctic Mountains, Antarctica. Tectonics 13, 818-836.

Flower, B.P., Kennett, J.P., 1994. The middle Miocene climatic transition: East Antarctic ice sheet development, deep ocean circulation and global carbon cycling. Palaeogeography, palaeoclimatology, palaeoecology 108, 537-555.

Frakes, L.A., 1975. Paleoclimatic significance of some sedimentary components at Site 274. Initial Reports of the Deep Sea Drilling Project 28, 785-787.

Francis, J.E., Woolfe, K.J., Arnott, M.J., Barrett, P.J., 1994. Permian climates of the southern margins of Pangea: evidence from fossil wood in Antarctica. Pangea: Global Environments and Resources- Memoir 17, 275-282.

Francis, J.E., Hill, R.S., 1996. Fossil plants from the Pliocene Sirius Group, Transantarctic Mountains: Evidence for climate from growth rings and fossil leaves. Palaios 11, 389-396.

Francis, J.E., 2000. Fossil Wood from Eocene High Latitude Forests: Mcmurdo Sound, Antarctica. In: Stilwel, J.D., Feldman, R.M. (Eds.), Paleobiology and Paleoenvironments of Eocene Rocks: McMurdo Sound, East Antarctica. American Geophysical Union, Washington, D.C., pp. 253-260.

Gagosian, R.B., Peltzer, E.T., 1986. The importance of atmospheric input of terrestrial organic material to deep sea sediments. Organic Geochemistry 10, 661-669.

Goodge, J.W., Myrow, P., Williams, I.S., Bowring, S.A., 2002. Age and provenance of the Beardmore Group, Antarctica: constraints on Rodinia supercontinent breakup. The Journal of geology 110, 393-406.

Gough, M.A., Rowland, S.J., 1990. Characterization of unresolved complex mixtures of hydrocarbons in petroleum. Nature 344, 648-650.

Gough, M.A., Rhead, M.M., Rowland, S.J., 1992. Biodegradation studies of unresolved complex mixtures of hydrocarbons: model UCM hydrocarbons and the aliphatic UCM. Organic Geochemistry 18, 17-22.

Grimalt, J., Albaigés, J., Al-Saad, H.T., Douabul, A.A.Z., 1985. n-Alkane distributions in surface sediments from the Arabian Gulf. Naturwissenschaften 72, 35-37.

Grimalt, J., Albaigés, J., 1987. Sources and occurrence of C_{12}-C_{22} n-alkane distributions with even carbon-number preference in sedimentary environments. Geochimica et Cosmochimica Acta 51, 1379-1384.

Hambrey, M.J., Barrett, P.J. 1993. Cenozoic sedimentary and climatic record, Ross Sea region, Antarctica. In: Kennett, J.P., Warnke, D.A. (Eds.) The Antarctic Paleoenvironment: A Perspective on Global Change: Part Two, American Geophysical Union, Washington, D.C., pp. 91-124.

Han, J., Calvin, M., 1969. Hydrocarbon distribution of algae and bacteria, and microbiological activity in sediments. Proceedings of the National Academy of Sciences 64, 436-443.

Hart, K.M., Szpak, M.T., Mahaney, W.C., Dohm, J.M., Jordan, S.F., Frazer, A.R., Allen, C.C.R., Kelleher, B.P., 2011. A bacterial enrichment study and overview of the extractable lipids from paleosols in the Dry Valleys, Antarctica: implications for future Mars reconnaissance. Astrobiology 11, 303-321.

Harwood, D.M., 1983. Diatoms from the Sirius Formation, Transantarctic Mountains. Antarctic Journal of the United States 18, 98-100.

Harwood, D.M., Levy, R.H., 2000. The McMurdo Erratics: introduction and overview. In: Stilwel, J.D., Feldman, R.M. (Eds.), Paleobiology and Paleoenvironments of Eocene Rocks: McMurdo Sound, East Antarctica, American Geophysical Union, Washington, D.C., pp. 1-18.

Herbert, T.D., Lawrence, K.T., Tzanova, A., Peterson, L.C., Caballero-Gill, R., Kelly, C.S., 2016. Late Miocene global cooling and the rise of modern ecosystems. Nature Geoscience 9, 843-847.

Inglis, G. N., Naafs, B. D. A., Zheng, Y., McClymont, E. L., Evershed, R. P., Pancost, R. D., 2018. Distributions of geohopanoids in peat: Implications for the use of hopanoid-based proxies in natural archives. Geochimica et Cosmochimica Acta 224, 249-261.

Kawamura, K., Ishimura, Y., Yamazaki, K., 2003. Four years' observations of terrestrial lipid class compounds in marine aerosols from the western North Pacific. Global Biogeochemical Cycles 17, 3-1-3-19.

Kemp, E.M., 1975. Palynology of Leg 28 drill sites, Deep Sea Drilling Project. Initial Reports of the Deep Sea Drilling Project 28, 599-623.

Kemp, E.M., Barrett, P. J., 1975. Antarctic glaciation and early Tertiary vegetation. Nature 258, 507-508.

Kraus, C., 2016. Oligocene to early Miocene glacimarine sedimentation of the central Ross Sea, and implications for the evolution of the West Antarctic Ice Sheet (Unpublished Masters Thesis). Victoria University of Wellington, New Zealand.

Kvenvolden, K.A., Rapp, J.B., Golan-Bac, M., Hostettler, F.D., 1987. Multiple sources of alkanes in Quaternary oceanic sediment of Antarctica. Organic geochemistry 11, 291-302.

884 Lehtonen, K., Ketola, M., 1993. Solvent-extractable lipids of Sphagnum, Carex, Bryales and Carex-
885 Bryales peats: content and compositional features vs peat humification. Organic
886 Geochemistry 20, 363-380.
887 Levy, R.H., Harwood, D.M., 2000. Tertiary marine palynomorphs from the McMurdo Sound erratics,
888 Antarctica. In Stilwel, J.D., Feldman, R.M. (Eds.), Paleobiology and Paleoenvironments of
889 Eocene Rocks: McMurdo Sound, East Antarctica, American Geophysical Union, Washington,
890 D.C., pp. 183-242.
891 Levy, R., Harwood, D., Florindo, F., Sangiorgi, F., Tripati, R., von Eynatten, H., Gasson, E., Kuhn.
892 G., Tripati, A., DeConto, R., Fielding, C., Field, B., Golledge, N., McKay, R., Naish, T., Olney,
893 M., Pollard, D., Schouten, S., Talarico, F., Warny, S., Willmott, V., Acton, G., Panter, K.,
894 Paulsen, T., Taviani, M., SMS Science Team, 2016. Antarctic ice sheet sensitivity to
895 atmospheric CO_2 variations in the early to mid-Miocene. Proceedings of the National Academy
896 of Sciences 113, 3453-3458.
897 Lewis, A.R., Marchant, D.R., Kowalewski, D.E., Baldwin, S.L., Webb, L.E., 2006. The age and
898 origin of the Labyrinth, western Dry Valleys, Antarctica: Evidence for extensive middle
899 Miocene subglacial floods and freshwater discharge to the Southern Ocean. Geology 34, 513-
900 516.
901 Lewis, A.R., Marchant, D.R., Ashworth, A.C., Hemming, S.R., Machlus, M.L., 2007. Major middle
902 Miocene global climate change: Evidence from East Antarctica and the Transantarctic
903 Mountains. Geological Society of America Bulletin 119, 1449-1461.
904 Lewis, A.R., Marchant, D.R., Ashworth, A.C., Hedenäs, L., Hemming, S.R, Johnson, J.V., Leng,
905 M.J., Machlus, M.L., Newton, A.E., Raine, J.I., Willenbring, J.K., Williams, M., Wolfe, A.P.,
906 2008. Mid-Miocene cooling and the extinction of tundra in continental Antarctica. Proceedings
907 of the National Academy of Sciences 105, 10676-10680.
908 Lewis, A.R., Ashworth, A.C., 2016. An early to middle Miocene record of ice-sheet and landscape
909 evolution from the Friis Hills, Antarctica. Geological Society of America Bulletin 128, 719-
910 738.
911 Luyendyk, B.P., Sorlien, C.C., Wilson, D.S., Bartek, L.R., Siddoway, C.S., 2001. Structural and
912 tectonic evolution of the Ross Sea rift in the Cape Colbeck region, Eastern Ross Sea,
913 Antarctica. Tectonics 20, 933-958.
914 Madureira, L.A., Piccinini, A., 1999. Lipids as indicators of paleoclimatic changes, II: terrestrial
915 biomarkers. Revista Brasileira de Oceanografia 47, 115-125.
916 Marchant, D.R., Denton, G.H., 1996. Miocene and Pliocene paleoclimate of the Dry Valleys region,
917 southern Victoria Land: a geomorphological approach. Marine Micropaleontology 27, 253-271.
918 Marchant, D.R., Denton, G.H., Swisher, C.C., Potter, N., 1996. Late Cenozoic Antarctic paleoclimate
919 reconstructed from volcanic ashes in the Dry Valleys region of southern Victoria
920 Land. Geological Society of America Bulletin 108, 181-194.

Martin, A.P., Cooper, A.F., Dunlap, W.J., 2010. Geochronology of Mount Morning, Antarctica: two-phase evolution of a long-lived trachyte-basanite-phonolite eruptive center. Bulletin of Volcanology 72, 357-371.

Matsumoto, G.I., Funaki, M., Machihara, T., Watanuki, K., 1986. Alkanes and alkanoic acids in the Beacon Supergroup samples from the Allan Hills and the Carapace Nunatak in Antarctica. Memoirs of National Institute of Polar Research. Special issue 43, 149-158.

Matsumoto, G. I., Machihara, T., Suzuki, N., Funaki, M., Watanuki, K., 1987. Steranes and triterpanes in the Beacon Supergroup samples from southern Victoria Land in Antarctica. Geochimica et Cosmochimica Acta 51, 2663-2671.

Matsumoto, G.I., Akiyama, M., Watanuki, K., Torii, T., 1990a. Unusual distributions of long-chain n-alkanes and n-alkenes in Antarctic soil. Organic Geochemistry 15, 403-412.

Matsumoto, G. I., Hirai, A., Hirota, K., Watanuki, K., 1990b. Organic geochemistry of the McMurdo dry valleys soil, Antarctica. Organic Geochemistry 16, 781-791.

Matsumoto, G.I., Honda, E., Sonoda, K., Yamamoto, S., Takemura, T., 2010. Geochemical features and sources of hydrocarbons and fatty acids in soils from the McMurdo Dry Valleys in the Antarctic. Polar Science 4, 187-196.

McKay, R., Browne, G., Carter, L., Cowan, E., Dunbar, G., Krissek, L., Naish, T., Powell, R., Reed, J., Talarico, F., Wilch, T., 2009. The stratigraphic signature of the late Cenozoic Antarctic Ice Sheets in the Ross Embayment. Geological Society of America Bulletin 121, 1537-1561.

McKay, R., Naish, T., Carter, L., Riesselman, C., Dunbar, R., Sjunneskog, C., Winter, D., Sangiorgi, F., Warren, C., Pagini, M., Schouten, S., Willmott, V., Levy, R., DeConto R., Powell, R. D., 2012. Antarctic and Southern Ocean influences on Late Pliocene global cooling. Proceedings of the National Academy of Sciences 109, 6423-6428.

Mackenzie, A. S., Patience, R. L., Maxwell, J. R., Vandenbroucke, M., Durand, B., 1980. Molecular parameters of maturation in the Toarcian shales, Paris Basin, France—I. Changes in the configurations of acyclic isoprenoid alkanes, steranes and triterpanes. Geochimica et Cosmochimica Acta 44, 1709-1721.

Meyers, P.A., Ishiwatari, R., 1993. Lacustrine organic geochemistry—an overview of indicators of organic matter sources and diagenesis in lake sediments. Organic geochemistry 20, 867-900.

Mildenhall, D.C., 1989. Terrestrial palynology. In: Barrett, P.J. (Ed.), Antarctic Cenozoic history from the CIROS-1 drillhole, McMurdo Sound. DSIR Publishing, Wellington, New Zealand, pp. 119-127.

Miller, M.C., McCave, I.N., Komar, P., 1977. Threshold of sediment motion under unidirectional currents. Sedimentology 24, 507-527.

Moossen, H., Bendle, J., Seki, O., Quillmann, U., Kawamura, K., 2015. North Atlantic Holocene climate evolution recorded by high-resolution terrestrial and marine biomarker records. Quaternary Science Reviews 129, 111-127.

Morin, R.H., Williams, T., Henrys, S.A., Magens, D., Niessen, F., Hansaraj, D., 2010. Heat flow and hydrologic characteristics at the AND-1B borehole, ANDRILL McMurdo Ice Shelf Project, Antarctica. Geosphere 6, 370-378.

Naish, T.R., Barrett, P.J., Dunbar, G.B., Woolfe, K.J., Dunn, A.G., Henrys, S.A., Claps, M., Powell, R.D., Fielding, C.R., 2001. Sedimentary cyclicity in CRP drillcore, Victoria Land Basin, Antarctica. Terra Antarctica 8, 225-244.

Naish, T., Powell, R., Levy, R., Wilson, G., Scherer, R., Talarico, F., Krissek, L., Niessen, F., Pompilio, M., Wilson, T., Carter, L., DeConto, R., Huybers, P., McKay, R., Pollard, D., Ross, J., Winter, D., Barrett, P., Browne, G., Cody, R., Cowan, E., Crampton, J., Dunbar, G., Dunbar, N., Florindo, F., Gebhardt, C., Graham, I., Hannah, M., Hansaraj, D., Harwood, D., Helling, D., Henrys, S., Hinnov, L., Kuhn, G., Kyle, P., Läufer, A., Maffioli, P., Magens, D., Mandernack, K., McIntosh, W., Millan, C., Morin R., Ohneiser, C., Paulsen, T., Persico, D., Raine, I., Reed, J., Riesselman, C., Sagnotti, L., Schmitt, D., Sjunneskog, C., Strong, P., Taviani, M., Vogel, S., Wilch T., Williams, T., 2009. Obliquity-paced Pliocene West Antarctic ice sheet oscillation. Nature 458, 322-328.

Ourisson, G., Albrecht, P., 1992. Hopanoids. 1. Geohopanoids: the most abundant natural products on Earth? Accounts of Chemical Research 25, 398-402.

Peters, K. E., Moldowan, J. M., 1991. Effects of source, thermal maturity, and biodegradation on the distribution and isomerization of homohopanes in petroleum. Organic geochemistry 17, 47-61.

Pole, M., Hill, B., Harwood, D., 2000. Eocene plant macrofossils from erratics, McMurdo Sound, Antarctica. In: Stilwel, J.D., Feldman, R.M. (Eds.), Paleobiology and Paleoenvironments of Eocene Rocks: McMurdo Sound, East Antarctica, American Geophysical Union, Washington, D.C., pp. 243-251.

Powell, R., Krissek, L.A., Van der Meer, J., 2000. Preliminary depositional environmental analysis of CRP-2/2A, Victoria Land Basin, Antarctica: palaeoglaciological and palaeoclimatic inferences. Terra Antarctica 7, 313-322.

Powell, R.D., Cooper, J.M., 2002. A glacial sequence stratigraphic model for temperate, glaciated continental shelves. Geological Society, London, Special Publications 203, 215-244.

Powell, R.D., Domack, E.W., 2002. Modern glacimarine environments. In: Menzies, J. (Ed.), Modern and Past Glacial Environments, Butterworth-Heinemann, Boston, pp. 361-390.

Poynter, J.G., Farrimond, P., Robinson, N., Eglinton, G., 1989. Aeolian-derived higher plant lipids in the marine sedimentary record: Links with palaeoclimate. In: Leinen, M., Sarnthein, M., (Eds.), Paleoclimatology and paleometeorology: modern and past patterns of global atmospheric transport, Springer, Netherlands, pp. 435-462

Prebble, J.G., Raine, J.I., Barrett, P.J., Hannah, M.J., 2006a. Vegetation and climate from two Oligocene glacioeustatic sedimentary cycles (31 and 24 Ma) cored by the Cape Roberts Project,

Victoria Land Basin, Antarctica. Palaeogeography, Palaeoclimatology, Palaeoecology 23, 41-57.

Prebble, J.G., Hannah, M.J., Barrett, P.J., 2006b. Changing Oligocene climate recorded by palynomorphs from two glacio-eustatic sedimentary cycles, Cape Roberts Project, Victoria Land Basin, Antarctica. Palaeogeography, Palaeoclimatology, Palaeoecology 231, 58-70.

Pross, J., Contreras, L., Bijl, P.K., Greenwood, D. R., Bohaty, S.M., Schouten, S., Bendle, J.A., Röhl, U., Tauxe, L., Raine, J.I., Huck, C.E., van de Flierdt, T., Jamieson, S.S.R., Stickley, C.E., van de Scootbrugge, B., Escutia, C., Brinkhuis, H., Integrated Ocean Drilling Program Expedition 318 Scientists, 2012. Persistent near-tropical warmth on the Antarctic continent during the early Eocene epoch. Nature 488, 73-77.

Rees-Owen, R.L., Gill, F.L., Newton, R.J., Ivanović, R.F., Francis, J.E., Riding, J.B., Vane, C.H., dos Santos, R.A.L., 2018. The last forests on Antarctica: Reconstructing flora and temperature from the Neogene Sirius Group, Transantarctic Mountains. Organic Geochemistry doi.org/10.1016/j.orggeochem.2018.01.001.

Ribecai, C., 2007. Early Jurassic miospores from Ferrar Group of Carapace Nunatak, South Victoria Land, Antarctica. Review of Palaeobotany and Palynology 144, 3-12.

Rohmer, M., Bouvier-Nave, P., Ourisson, G., 1984. Distribution of hopanoid triterpenes in prokaryotes. Microbiology 130, 1137-1150.

Sachse, D., Radke, J., Gleixner, G., 2006. δD values of individual n-alkanes from terrestrial plants along a climatic gradient–Implications for the sedimentary biomarker record. Organic Geochemistry 37, 469-483.

Sackett, W.M., Poag, C.W., Eadie, B.J., 1974. Kerogen recycling in the Ross Sea, Antarctica. Science 185, 1045-1047.

Sandroni, S., Talarico, F., 2004. Petrography and provenance of basement clasts in CIROS-1 core, McMurdo Sound, Antarctica. Terra Antarctica 11, 93-114.

Sandroni, S., Talarico, F.M., 2011. The record of Miocene climatic events in AND-2A drill core (Antarctica): Insights from provenance analyses of basement clasts. Global and Planetary Change 75, 31-46.

Schefuß, E., Ratmeyer, V., Stuut, J.B.W., Jansen, J.H.F., Sinninghe Damsté, J.S., 2003. Carbon isotope analyses of n-alkanes in dust from the lower atmosphere over the central eastern Atlantic. Geochimica et Cosmochimica Acta 67, 1757-1767.

Schellekens, J., Buurman, P., Pontevedra-Pombal, X., 2009. Selecting parameters for the environmental interpretation of peat molecular chemistry–a pyrolysis-GC/MS study. Organic Geochemistry 40, 678-691.

Schellekens, J., Buurman, P., 2011. n-Alkane distributions as palaeoclimatic proxies in ombrotrophic peat: the role of decomposition and dominant vegetation. Geoderma 164, 112-121.

1030 Scherer, R., Hannah, M., Maffioli, P., Persico, D., Sjunneskog, C., Strong, C. P., Taviani, M., Winter,
1031 D., 2007. Palaeontologic characterisation and analysis of the AND-1B core, ANDRILL
1032 McMurdo Ice Shelf Project, Antarctica. Terra Antarctica 14, 223-254.
1033 Schröder, H., Paulsen, T., Wonik, T., 2011. Thermal properties of the AND-2A borehole in the
1034 southern Victoria Land Basin, McMurdo Sound, Antarctica. Geosphere 7, 1324-1330.
1035 Seifert, W. K., Moldowan, J. M., 1978. Applications of steranes, terpanes and monoaromatics to the
1036 maturation, migration and source of crude oils. Geochimica et Cosmochimica Acta 42, 77-95.
1037 Seifert, W. K., Moldowan, J. M., 1980. The effect of thermal stress on source-rock quality as
1038 measured by hopane stereochemistry. Physics and Chemistry of the Earth 12, 229-237.
1039 Shackleton, N.J., Kennett, J.P., 1975. Paleotemperature history of the Cenozoic and the initiation of
1040 Antarctic glaciation: oxygen and carbon isotope analyses in DSDP Sites 277, 279, and
1041 281. Initial reports of the deep sea drilling project 29, 743-755.
1042 Smellie, J.L., 2001. History of Oligocene erosion, uplift and unroofing of the Transantarctic
1043 Mountains deduced from sandstone detrital modes in CRP-3 drillcore, Victoria Land Basin,
1044 Antarctica. Terra Antarctica 8, 481-490.
1045 Strogen, D.P., Bland, K.J., 2011. Hydrocarbon Risk for Drilling on the Coulman High, GNS Science
1046 Consultancy Report Volume 2011/185, GNS Science, Lower Hutt, New Zealand.
1047 Strong, C. P., Webb, P. N., 2000. Oligocene and Miocene Foraminifera from CRP-2/2A, Victoria
1048 Land Basin, Antarctica. Terra Antarctica 7, 461-472.
1049 Sugden, D.E., Marchant, D.R., Denton, G.H., 1993. The case for a stable East Antarctic ice sheet: the
1050 background. Geografiska Annaler. Series A. Physical Geography 75, 151-154.
1051 Sugden, D., Denton, G., 2004. Cenozoic landscape evolution of the Convoy Range to Mackay Glacier
1052 area, Transantarctic Mountains: onshore to offshore synthesis. Geological Society of America
1053 Bulletin 116, 840-857.
1054 Talarico, F., Sandroni, S., Fielding, C. R., Atkins, C., 2000. Variability, petrography and provenance
1055 of basement clasts in core from CRP-2/2A, Victoria Land Basin, Antarctica. Terra Antarctica 7,
1056 529-544.
1057 Talbot, H. M., Farrimond, P., 2007. Bacterial populations recorded in diverse sedimentary
1058 biohopanoid distributions. Organic Geochemistry 38, 1212-1225.
1059 The Shipboard Scientific Party, 1975a. Shipboard Site Reports: Sites 270, 271, 272. Initial Reports of
1060 the Deep Sea Drilling Project 28, 211-334.
1061 The Shipboard Scientific Party, 1975b. Shipboard Site Reports: Site 274. Initial Reports of the Deep
1062 Sea Drilling Project 28, 369-433.
1063 Tissot, B.P., Welte, D.H., 1984. Petroleum Formation and Occurrence (2nd ed.). Springer-Verlag,
1064 Berlin Heidelberg.
1065 Truswell, E.M., Drewry, D.J., 1984. Distribution and provenance of recycled palynomorphs in
1066 surficial sediments of the Ross Sea, Antarctica. Marine Geology 59, 187-214.

1067 Venkatesan, M.I., 1988. Organic geochemistry of marine sediments in Antarctic region: marine lipids
1068 in McMurdo Sound. Organic Geochemistry 12, 13-27.
1069 Vogts, A., Moossen, H., Rommerskirchen, F., Rullkötter, J., 2009. Distribution patterns and stable
1070 carbon isotopic composition of alkanes and alkan-1-ols from plant waxes of African rain forest
1071 and savanna C_3 species. Organic Geochemistry 40, 1037-1054.
1072 Warny, S., Askin, R.A., Hannah, M.J., Mohr, B.A., Raine, J.I., Harwood, D.M., Florindo, F., 2009.
1073 Palynomorphs from a sediment core reveal a sudden remarkably warm Antarctica during the
1074 middle Miocene. Geology 37, 955-958.
1075 Webb, P.N., Harwood, D.M., McKelvey, B.C., Mercer, J.H., Stott, L.D., 1984. Cenozoic marine
1076 sedimentation and ice-volume variation on the East Antarctic craton. Geology 12, 287-291.
1077 Whittaker, J.M., Müller, R.D., 2006. Seismic stratigraphy of the Adare Trough area,
1078 Antarctica. Marine geology 230, 179-197.
1079 Wilson, D.S., Luyendyk, B.P., 2009. West Antarctic paleotopography estimated at the Eocene-
1080 Oligocene climate transition. Geophysical Research Letters 36, L16302,
1081 doi:10.1029/2009GL039297.
1082 Zhou, W., Xie, S., Meyers, P.A., Zheng, Y., 2005. Reconstruction of late glacial and Holocene
1083 climate evolution in southern China from geolipids and pollen in the Dingnan peat
1084 sequence. Organic Geochemistry 36, 1272-1284.